Institute of Forest Ecology, Department of Forest- and Soil Sciences, University of Natural Resources and Life Sciences, Vienna

---

Effects of Ungulate Herbivores on Post-Disturbance Forest Soil Carbon Dynamics in the Northern Calcareous Alps

Thesis submitted in partial fulfillment of the requirements for the degree of

Diplomingenieur

submitted by

David Keßler

Supervisor

Ao.Univ.Prof. Dipl.-Ing. Dr.nat.techn. Klaus Katzensteiner

Co-supervisor

Dipl.-Ing. Dr.nat.techn. Mathias Mayer

Institute of Forest Ecology, BOKU

Vienna, March 2018

Danksagung

Herzlichst bedanken möchte ich mich bei Ao.Univ.Prof. Dipl.-Ing. Dr.nat.techn. Klaus Katzensteiner und Dipl.-Ing. Dr.nat.techn. Mathias Mayer für die äußerst gute Betreuung, die nette, geduldige und wertvolle Unterstützung und die Vielzahl hilfreicher Anregungen während meiner Masterarbeit sowie meiner Projektmitarbeit in den vergangenen Jahren.

Weiters gilt auch dem Stab des Instituts für Waldökologie großer Dank, insbesondere Ao.Univ.Prof. Dipl.-Ing. Dr.nat.techn. Torsten Berger, Sigrid Gubo, B.A., Dr.nat.techn. Bradley Matthews, MSc und Dipl.-Ing. Martin Wresowar.

Dipl.-Ing. Alois Simon danke ich für die Erschließung der Tiroler Landschaft.

Besonderer Dank gebührt meinen lieben Eltern für die Unterstützung und den Rückhalt über die Jahre.

Zudem auch besten Dank an meine Freunde und Geschwister.

Table of Contents

Danksagung i
Table of Contents ii
List of Figures v
List of Acronyms and Abbreviations viii
1. Introduction 1
2. Materials and Methods 5
2.1 Study Sites 5
2.2 Experimental design 7
2.3 Soil CO_2 efflux, heterotrophic respiration, autotrophic respiration and soil microclimate 9
2.4 Site parameters 11
2.5 Statistical analysis 14
2.5.1 Calculation of soil CO_2 efflux, heterotrophic respiration, autotrophic respiration and soil microclimate 14
2.5.2 Site parameters controlling CO_2 efflux 18
2.5.3 Spatial correlation and mapping of CO_2 efflux 18
3. Results 21
3.1 Effects of fencing on soil CO_2 efflux, heterotrophic respiration, autotrophic respiration and soil microclimate 21
3.2 Site parameters controlling CO_2 efflux 30
3.3 Spatial correlation and mapping of CO_2 efflux 35
4. Discussion 39
4.1 Effects of fencing on soil CO_2 efflux, R_h, R_a and soil microclimate 39
4.2 Site parameters controlling CO_2 efflux 45
4.3 Spatial correlation and mapping of CO_2 efflux 48
5. Conclusion 49
6. Abstract 50
7. Zusammenfassung 51
8. References 53
9. Appendix 60

List of Tables

Table 1: Distribution of the root exclusion plots, the number of plots for measuring R_s and the additional plots of the geometrical stratified sampling scheme for the locations and the treatments at the Hoellengebirge site and the Reutte site. 10

Table 2: Soil types of the research site at the Reutte site and their characteristics, classified according to the *Austrian Soil Classification* (ASC) and the *World Reference Base for Soil Resources* (WRB) (modified after Scheffer and Schachtschabel, 2016 and Nestroy et al., 2011). 12

Table 3: Humus forms of the research site at the Reutte site and their characteristics classified according to the *Austrian Soil Classification* (ASC) and the *European Humus Forms Reference Base* (EHFRB) (modified after Nestroy et al., 2011). 13

Table 4: Summary of the treatment specific regression model of soil respiration after equation 1 ($R_s = \beta_1 e^{(\beta 2\ Ts)}$) in relation to soil temperature, where R_s is the CO_2-efflux (µmol CO_2 m^{-2} s^{-1}) and T_s is the soil temperature (°C). Q_{10} is the temperature sensitivity calculated by means of equation 2 ($Q_{10} = e^{\beta 10}$) and R_{10} is the basal soil respiration at 10 °C calculated by means of equation 3 ($R_{10} = \beta_1 e^{(\beta 2\ 10)}$). 26

Table 5: Summary of the plot specific mixed effect model of soil respiration after equation 8 ($Ln(Rs) = \beta_1 + \beta_2 T_s + \beta_3 VWC_s$) in dependence to soil temperature and soil moisture where R_s is the CO_2 efflux (µmol CO_2 m^{-2} s^{-1}), β_1, β_2 and β_3 model coefficients, Ts the soil temperature (°C) and VWC_s the volumetric water (%) content. 27

Table 6: Summaries of two sample t-tests and ANOVA comparing R_{10} in relation to different factor variables and summary statistics of a linear models describing the relationship of R_{10} to different site and topographic variables and statistical summaries of two way ANOVA and ANCOVA and linear models to account for interactions between treatments and site parameters with respect to R_{10}. Significant correlations are pointed out by bolded p-values ($p < 0.05$). 32

Table 7: Characterization of each treatment with respect to the assessed site parameters. Represented are the identified numbers of each humus form, soil type, soil group and microtopography and also the averages of layer depths of soil horizons (cm), soil cover (%), vegetation cover (%), canopy closure (%), functional groups (%), slope (°), aspect (°) and elevation a.s.l. (m). 34

Table 8: Variogram summaries for the measurement campaigns 4, 5 & 6, which include the plots of the SRS and the geometrical stratified scheme. Spatial correlations of R_s were modeled by means of a spherical model. 35

Table A1: Summary statistics of campaign wise measured soil respiration (R_s), soil temperature (T_s) and volumetric water content (VWC_s) for the whole site, the unfenced treatment (UF) and the fenced treatment (FE) at the Hoellengebirge. 61

Table A2: Summary statistics of campaign wise measured soil respiration (R_s), soil temperature (T_s) and volumetric water content (VWC_s) for the whole site and the unfenced treatment (UF) at the Reutte site. 62

Table A3: Summary statistics of campaign wise measured soil respiration (R_s), soil temperature (T_s) and volumetric water content (VWC_s) for the fenced site (FE) and the mature stand (MS) at the Reutte site. 63

Table A4: Treatment-specific effects of fencing on soil temperature (T_s (°C)), soil volumetric water content (VWC_s (%)) and soil CO_2 efflux (R_s (µmol CO_2 m^{-2} s^{-1})), as assessed by t-tests and Tukey´s HSD tests with mixed model structure. 64

Table A5: Treatment specific effects of fencing on autotrophic (R_a (µmol CO_2 m^{-2} s^{-1})) and heterotrophic respiration (R_h (µmol CO_2 m^{-2} s^{-1})), as assessed by t-tests and Tukey´s HSD tests with mixed model structure. 64

Table A6: Summary statistics of campaign wise modeled soil respiration (R_{model}), soil temperature (T_{model}) and volumetric water content (VWC_{model}) for the whole site, the unfenced treatment (UF) and the fenced treatment (FE) at the Hoellengebirge. 67

Table A7: Summary statistics of campaign wise modeled soil respiration (R_{model}), soil temperature (T_{model}) and volumetric water content (VWC_{model}) for the whole site and the unfenced treatment (UF) at the Reutte site. 68

Table A8: Summary statistics of campaign wise modeled soil respiration (R_{model}), soil temperature (T_{model}) and volumetric water content (VWC_{model}) for the fenced treatment (FE) and the mature stand (MS) at the Reutte site. 69

Table A9: Modeled amount of total emitted carbon (gC m^{-2}) for the different locations and treatments during the measurement period from 18.06.2016 to 24.10.2016 70

Table A10: Summary statistics of post-hoc Tukey tests for a further subdivision of the factor variables "Stratum" and "Humus form" and two sample t-test for the factor variable "soil group" with respect to R_{10}. Significant p-values are highlighted in bold ($p < 0.05$) 70

Table A11: Summary statistics of post-hoc Tukey tests for a further subdivision of the factor "Canopy Cover" and "Functional group" with respect to measured soil temperature. Significant p-values are highlighted in bold ($p < 0.05$) 71

List of Figures

Fig. 1: Representative description of the soil organic carbon (SOC) cycle on post-disturbance forest sites of (b) unfenced and (b) fenced treatments at an early stage of succession. Arrows indicate the main mechanisms of the soil organic carbon cycle and the dominant changes (bold arrows and size of letters) of the components of soil respiration (R_s) between the treatments, differentiated in its autotrophic (R_a) and heterotrophic (R_h) components. 3

Fig. 2 : Locations and impressions of the selected research sites at the Reutte site (a & b) and at the Hoellengebirge (c & d). 6

Fig. 3: Sampling scheme of the simple random plots (SRS) and the geometrical stratified sampling plots with different distance stages at the Reutte site. 8

Fig. 4 : Comparison of the Hoellengebirge site (a-c) and at the Reutte site (d-e) regarding average (mean +/- SE) CO_2 efflux (R_s) (a & d), soil temperature (b & f) and soil moisture (c & f) of the unfenced treatment (UF), the fenced treatment (FE) and the mature stand (MS) during the measurement period from May until end of October. Horizontal lines indicate the average of the respective variable during the measurement period (solid line = UF, dotted line = FE, dotdashed line = MS). 22

Fig. 5: Seasonal variations of (a) & (d) soil heterotrophic respiration (R_h), (b) & (e) soil autotrophic respiration rates (R_a) and (c) & (f) the contribution of autotrophic respiration to the total respiration (RaC) at the Hoellengebirge site and at the Reutte site, respectively. The data reflect the average values (mean ± SE) of each measurement campaign between the period from end of April to end of October 2016. In cases when R_h were higher than R_s, R_a was set to be zero. 24

Fig. 6: Total soil respiration (R_s) (a&c) and heterotrophic respiration (R_h) (b&d) in dependence to soil temperature during the measurement period from mid June to end of October, separated by Treatment (dotted = UF, solidline = FE) for the research sites at the Hoellengebirge site (a & b) and at the Reutte site (c & d). Regression lines were fitted by means of euqation 1 ($R_s = \beta_1 e^{(\beta 2\ Ts)}$). 25

Fig. 7: R_{model} (a & d), T_{model} (b & e) and VWC_{model} (c & f) after equation 6-8 over the measurement period from mid 18.06.2016 until 24.10.2016 for the fenced (green), unfenced (red) and the mature stand (dark green) treatment at the Hoellengebirge site and at Reutte site. 28

Fig. 8: Comparison of the modeled amount of emitted C during the measurement period from 18.06.2016 to 24.10.2016 in the unfenced (UF) and the fenced (FE) treatment at the Hoellengebirge site (a) and at the Reutte site (b). R_s, R_h and R_a represent the total soil respiration, heterotrophic and autotrophic respiration, respectively. R_a was calculated by the subtraction of R_s by R_h. Error bars represent the standard error of the mean. 29

Fig. 9: Box and whisker plots of R_{10} depending on the variables "treatment", "soil group" and "humus form". Different letters indicate significant differences between factors levels on a site scale ($p < 0.05$). 33

Fig. 10: Variograms of R_s for the measurement campaigns (a-c) including the plots of the simple random scheme and the geometrical stratified sampling scheme. Spatial correlation of the measured R_s were modeled by means of a spherical model. 36

Fig. 11: Ordinal kriging map for the measured and interpolated soil temperature (T_s) (a) and soil respiration (R_s) (b) for the fourth measurement campaign at the 22./23.08.2016. The green line indicates the fenced treatment (RF03), the brown line the mature stand (MS) and the in-between area the unfenced treatment (RU03). 37

Fig. 12: Ordinal kriging map for the measured and interpolated soil temperature(T_s) (a) and soil respiration (R_s) (b) for the fifth measurement campaign at the 22./23.09.2016. The green line indicates the fenced treatment (RF03), the brown line the mature stand (MS) and the in-between area the unfenced treatment (RU03). 37

Fig. 13: Ordinal kriging map for the measured and interpolated soil temperature (T_s) (a) and soil respiration (R_s) (b) for the sixth measurement campaign at the 21./22.10.2016. The green line indicates the fenced treatment (RF03), the brown line the mature stand (MS) and the in-between area the unfenced treatment (RU03). 38

Fig. A1: Model diagnostics of the mixed effects model to predict the soil respiration (µmol CO_2 m^{-2} s^{-1}) in dependence to soil temperature and soil moisture at the specific sampling plots after Equ. 8 ($Ln(Rs) = \beta 1 + \beta 2\ Ts + \beta 3\ VWCs$) (a & b) Show a QQ - plot of the residuals normality distribution of the model, (c & d) the homoscedasticity plot for the site at the Hoellengebirge and at Reutte, respectively. 65

Fig. A2: Model diagnostics of the ME effects model to predict the temperature at 5 cm (°C) at the specific sampling plots after Equ. 6 ($T_s = \beta_1 + \beta_2\ T_{cont} + \beta_3\ T_{cont}^2$). Quadratic term was included to account for a potential shading effect. (a & b) Show a QQ - plot of the residual normality distribution of the Model, (c & d) the homoscedasticity plot for the site at the Hoellengebirge and at Reutte site, respectively. 65

Fig. A3: Model diagnostics of the ME effects model to predict the soil moisture at the specific sampling plots after Equ. 7 ($VWC_s = \beta_1 + \beta_2\ VWC_{cont}$). (a &b) Show a QQ - plot of the residuals normality distribution of the Model, (c & d) the homoscedasticity plot for the site at the Hoellengebirge and at Reutte, respectively. 66

List of Equations

Equation 1: $R_s = \beta_1 e^{(\beta_2 T_s)}$ 14

Equation 2: $Q_{10} = e^{\beta 10}$ 15

Equation 3: $R_{10} = \beta_1 e^{(\beta_2 10)}$ 15

Equation 4: $Rs = R10\ Q10^{(\frac{Ts-10}{10})}$ 15

Equation 5: $CO_2\ efflux = -0.11 + 0.02\ VWC_s - 0.0002\ VWC_s^2$ 16

Equation 6: $T_s = \beta_1 + \beta_2 T_{cont} + \beta_3 T_{cont}^2$ 17

Equation 7: $VWC_s = \beta_1 + \beta_2 VWC_{cont}$ 17

Equation 8: $Ln(Rs) = \beta_1 + \beta_2 T_s + \beta_3 VWC_s$ 17

Equation 9: $\gamma(h) = \frac{1}{2\,N(h)} \sum_{i=1}^{N(h)} [z(x_i) - z(x_i + h)]^2$ 19

Equation 10: $\gamma h = \begin{cases} c_0 + c\left[\frac{3h}{2a} - \frac{1}{2}\left(\frac{h}{a}\right)\right] \\ c_0 + c \end{cases} \begin{matrix} for\ h \le a, \\ k \\ for\ h > a \end{matrix}$ 19

Equation 11: $nc = \frac{c_0}{c_0 + c}$ 20

List of Acronyms and Abbreviations

AIC: Akaike Information Criterion
C: Carbon
CO_2: Carbon dioxide
CV: Coefficient of variation
FE: Fenced treatments
HF07: Fenced treatment at the Hoellengebirge site
HU07: Unfenced treatment at the Hoellengebirge site
ME: Mixed effect model
MS: Mature stand at the Reutte site
R_a: Autotrophic respiration
RaC: Percentage of autotrophic respiration on the total soil respiration
RF03: Fenced treatment at the Reutte site
R_h: Heterotrophic respiration
RMSE: Root mean square error
R_s: Soil respiration
R_{model}: Modeled soil respiration
RU03: Unfenced treatment at the Reutte site
SD: Standard deviation
SE: Standard error of the mean
SOC: Soil organic carbon
SRS: Simple random scheme
T_{cont}: Continuously measured soil temperature
T_{model}: Modelled soil temperature
T_s: Soil temperature at a depth of 5 cm
UF: Unfenced treatments
VWC_{cont}: Continuously measured volumetric water content
VWC_{model}: Modelled volumetric water content
VWC_s: Volumetric water content at a soil depth of 0-7 cm

1. Introduction

Soils represent the largest terrestrial carbon (C) pool with an global stock of about 1500 Pg C (Scharlemann et al., 2014). Soil organic carbon (SOC) reflect the balance between C inputs (organic residues of animals and plants) and C outputs including mineralization of organic complexes as well as erosion losses and leaching (Tian et al., 2015). With about 98 Pg C yr^{-1} the global carbon dioxide (CO_2) efflux from soils is the largest source of CO_2 in terrestrial ecosystems, more than 10 times higher than emitted by fossil fuel combustion (Bond-Lamberty and Thomson, 2010, Reichstein and Beer, 2008). Thereby, soil respiration (R_s) represents the main respiratory C efflux (~60% of ecosystem respiration) in most forest ecosystems (Yuste et al., 2005, Janssens et al., 2001). Soil respiration can be differentiated in two components. First, autotrophic respiration (R_a) from internal plant metabolism and subsequent root respiration as well as root-associated respiration (mycorrhizal fungi and rhizosphere heterotrophs). Second, heterotrophic respiration (R_h) from organisms, which decompose organic matter originated from litter fall, dead woody debris, root turn-over, root exudation, fecal matter and dead organisms (Kirschbaum, 2001). The relative contribution of R_a to R_s varies among studies and investigated ecosystems and ranges from 10 to 90% (Subke et al., 2006, Hanson et al., 2000). The contribution of R_a to R_s (RaC) is about 50% in intact forest stands and 30-40% in temperate grasslands (Subke et al., 2006, Hanson et al., 2000). The lower RaC in grasslands can be related to a high litter quantity and quality of grasses which stimulates the heterotrophic community (Freschet et al., 2013, Hiltbrunner et al., 2013).

In general, temperate forest ecosystems act as carbon sinks. This can be attributed to photosynthetic C uptake and its storage in biomass and soil (Prietzel and Christophel, 2014, Gruneberg et al., 2014, Kirk, 2016, Thuille and Schulze, 2006). Stand replacing disturbances like windthrows, forest fires, insect infestations or harvests can drastically weaken the C sink strength of forest ecosystems (Amiro et al., 2010).

In Austria 75% of the forest areas where rejuvenation is urgently required are markedly affected by an inhibited natural regeneration, mainly caused by the high densities of ungulate herbivores (Prem, 2016). The extermination of natural predators and the feeding of these herbivores during the winter months impede natural regulation mechanisms of them (Fuller and Gill, 2001, BMLFUW, 2013). The good nutritional status has led to a decrease of the age when herbivores reach their sexual maturity, which is besides too low game shootings the main reason for the increase of their densities (Wildburger, 2005). This leads to a lack of

regeneration and therefore to a decrease of resilience of forest ecosystems, which also affects forest ecosystem services in general as well as the potential of forest ecosystems to act as carbon sink (Pröll et al., 2015, Vacik and Lexer, 2001, Reimoser, 2010, Prietzel and Christophel, 2014, Prietzel, 2008).

If tree regeneration after disturbance events fails, the first succession stage (bare soil) could be prolonged and a subsequent establishment of dense grass layers may additionally hamper the establishment of saplings and seedling (Mayer et al., 2017b, Pröll et al., 2015, Mayer et al., 2014). Mayer et al. (2014) found no changes in R_s on sites with failed tree regeneration 3 and 5 years after windthrow when compared to mature stands - despite a strong decline in R_a. This finding was attributed to increased R_h induced by higher ground insolation and subsequently higher temperatures. Such a temperature-related increase in R_h was also identified to significantly reduce SOC stocks after disturbance events (Mayer et al., 2017b). Moreover, Mayer et al. (2014) found a significant higher R_s at a post-disturbance site covered with dense grass vegetation when compared to a control stand. This pattern was explained by increased autotrophic respiration and input of easy decomposable litter and root exudates stimulating the heterotrophic community. Even underneath a dense grass layer SOC content in organic layers could be shown to be reduced when compared to undisturbed mature stands (Spielvogel et al., 2006). Mayer et al. (2017a) could show, if tree regeneration is successful, R_h tends to be similar compared to a mature stand, mainly caused by lower temperatures due to an existing canopy closure. Prietzel (2008) found significant lower SOC contents in the organic layer at forest stands with high browsing pressures and regeneration deficits when compared to a fenced forest stand. Furthermore, trampling damages by ungulates and wind as well as water erosion induced by the failed tree regeneration cause additional humus losses (Prietzel, 2008). Figure 1 visualizes the findings of aforementioned studies for an early phase of succession, when a dense grass layer has not been established. While figure 1a reflects the SOC cycle on a fenced treatment with successful tree regeneration (FE), figure 1b reflects the unfenced treatment with high browsing pressures (UF). Higher temperatures stimulate the mineralization of organic matter at the unfenced treatment, while the R_a and also the assimilated C from photosynthesis are reduced due to the sparse ground vegetation (Fig. 1b). This may lead to a higher R_s at the UF than in the FE and results in lower SOC stocks.

Regarding the presumed increase in the intensity and frequency of disturbance events due to climate change and discussions in context of the Paris Climate agreement, it is essential to understand how disturbance affect the soil carbon cycle and its underlying mechanisms

(Schelhaas et al., 2010, Seidl et al., 2014, Seidl et al., 2017, Lindroth et al., 2009) Nevertheless, studies comparing failed tree regeneration - caused by browsing pressures - and successful tree regeneration after disturbance events on R_s and its components are quite rare. Therefore, this is the first *in-situ* study investigating the effects of fencing and thus of excluded ungulate tree herbivory on R_s and its components of windthrow sites in the Northern Calcareous Alps.

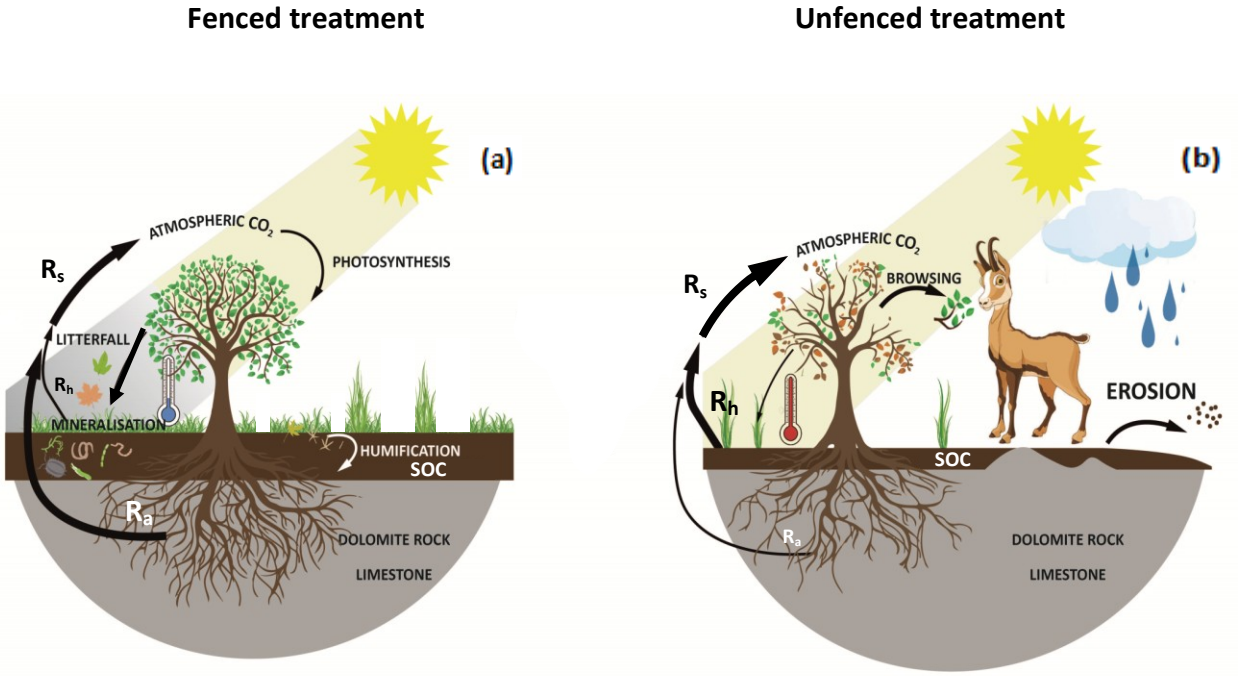

Fig. 1: Representative description of the soil organic carbon (SOC) cycle on post-disturbance forest sites of (a) fenced and (b) unfenced treatments at an early stage of succession. Arrows indicate the main mechanisms of the soil organic carbon cycle and the dominant changes (bold arrows and size of letters) of the components of soil respiration (R_s) between the treatments, differentiated in its autotrophic (R_a) and heterotrophic (R_h) components.

Hence, the study was designed under consideration of the following objectives:

(1) Effects of fencing on R_a, R_h and R_s
- Objectives: investigate the effect of fencing on the components of soil respiration (R_s, R_h, R_a)
  - Hypothesis 1: in an earlier stage of succession - when dense grass layers have not been established - the UF show lower R_a, but in later stages of succession - when a dense grass layer has already been established - R_a is higher in the UF.
  - Hypothesis 2: R_h in the UF is higher than in the FE and dominates Rs.
    Due to the missing canopy closure in the UF higher temperatures during vegetation period stimulate microbial activity.

(2) Modeling of soil respiration
- Objectives:
  - computation of plot specific soil respiration models to estimate the total amount of CO_2 emitted from the soil during the whole measurement period

(3) investigate the effect of site parameters on soil respiration
- Objectives:
  - investigate the influence of biotic and abiotic site parameters on R_s

(4) spatial dependencies and mapping
- Objectives:
  - explanation of the spatial variability and dependencies of soil respiration and possible changes with time to use it for geostatistical approaches (kriging).
  - creation of maps, for the visual assessment of spatio-temporal patterns of R_s to detect potential hot-spots.

2. Materials and Methods

2.1 Study Sites

The study took place in the Hoellengebirge mountain range, Upper Austria (47° 47′ 19′′ N, 13° 38° 21′′ E) and near the village of Reutte, Tyrol. (47° 27′ 27′′ N, 10° 40′ 12′′ E), located in the central and the western part of the Austrian Calcareous Alps, respectively (Fig. 2). The study site in the Hoellengebirge mountain range is a montane, south-west exposed mixed-forest at an altitude of around 1000 meters a.s.l.. The study site at the Reutte is a montane, south-east exposed and coniferous dominated forest site at an altitude of around 950 meters a.s.l.. In 2016, the annual precipitation and the average temperature were 1903 mm and 7.1 °C at the Hoellengebirge site. Annual values were interpolated for the elevation of the site using data from the climate stations "Feuerkogel" and "Bad Ischl" (ZAMG, 2017). At the Reutte site, the annual precipitation and the mean temperature in 2016 were 1351 mm and 8.6 °C. Annual values were measured at the climate station "Reutte" nearby the study site (ZAMG, 2017). The natural woodland community of both sites is dominated by *Picea abies, Abies alba* and *Fagus silvatica* (Kilian, 1994). The Hoellengebirge and the Reutte sites are similar regarding bedrock and soil conditions. The underlying bedrock consists of limestone ("Wettersteinkalk") and dolomite or of an paragenesis of both (Mayer et al., 2014, Cerny, 2000). Shallow soils like Histosols and Rendzic Leptosols dominate steeper sites, while Rendzic Cambic Leptosols and Chromic Cambisols dominate in accumulation zones (soil types according to the World Reference Base, (FAO, 2015)). Main humus forms are Mull, Moder and Tangel, classified according to the Austrian Soil Systematics (Nestroy, 2011) and the European Humus Forms Reference Base (Zanella, 2011). The Hoellengebirge site is managed by the Austrian Federal Forests, and the Reutte site is managed by a local community.

Both sites were destroyed by a stand-replacing windthrow event: the Hoellengebirge site in 2007 and the Reutte site in 2003. The extent of the damaged forest area is ~25 hectares and ~2 hectares at the Hoellengebirge site and at the Reutte site, respectively. At both sites, the timber (mainly the stem fraction) was removed after the disturbance event.

At both sites, a fence was established for ungulate exclusion and to observe the influence of browsing on tree regeneration. At the Hoellengebirge site the unfenced zone (abbreviated as HU07) has been reforested with European larch (*Larix decidua)* and Norway spruce (*Picea*

abies), while the fenced zone (HF07) at the Hoellengebirge, the unfenced (RU03) and the fenced zone (RF03) at the Reutte site have been reforested with European larch, Norway spruce, European silver fir (*Abies alba),* sycamore *(Acer pseudoplatanus),* rowan *(Sorbus aucuparia),* European beech *(Fagus sylvatica)* and Scots pine *(Pinus sylvestris).* At both UF, grasses *(Calamagrostis sp.)* are the dominating vegetation species.

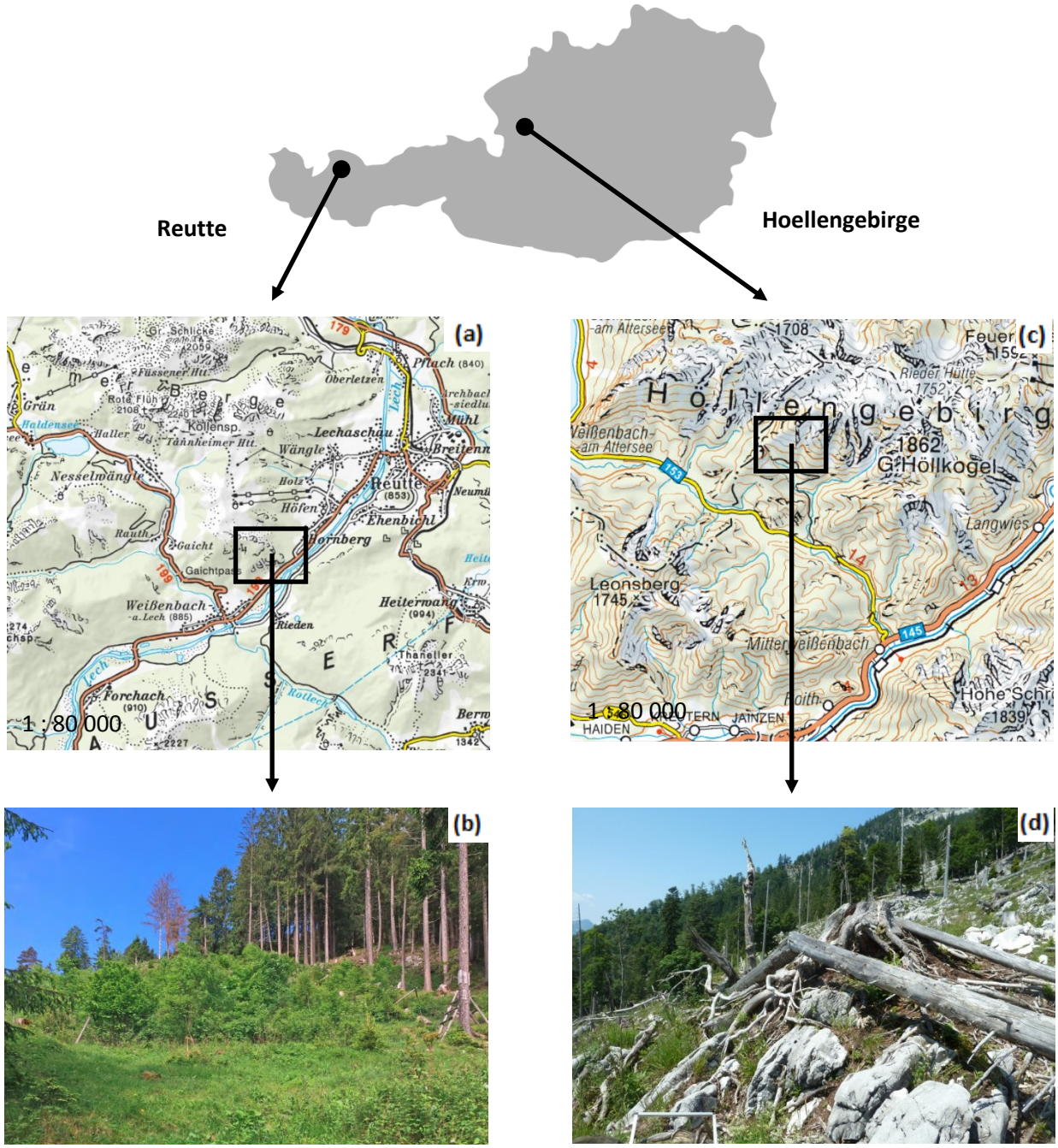

Fig. 2 : Locations and impressions of the selected research sites at the Reutte site (a & b) and at the Hoellengebirge (c & d).

2.2 Experimental design

At the Hoellengebirge site 23 and 16 plots were established at HU07 and HF07, respectively. The HU07 were part of an earlier experiment and were established in a nested (multi-level) sampling design in 2010 (for details see (Mayer et al., 2014)). The HF07 plots were randomly established along two slope line transects in 2015. Each transect line contained 8 plots (Table 1).

At the Reutte site, 8 plots at the adjacent mature stand (MS) and 16 plots at each RU03 and RF03 were established according to a simple random scheme (SRS) (Webster 2001). In order to conduct a geostatistical analysis, 105 plots were additionally established at the Reutte site in August 2016. Additional plots were established according to a geometrical stratified sampling scheme (Webster, 2001). The scheme of a basic grid of 20 x 20 meters was further subdivided into 10 x 10 m, 5x5 m, 2.5 x 2.5 m and 1.25 x 1.25 meter grids respectively (Fig. 2). This was carried out for each treatment and microtopographic condition (accumulation and loss) to reduce the within-treatment variance (Webster, 2001). Therefore, the Reutte site was covered by 40 sampling plots of the SRS and 105 sampling plots of the stratified sampling scheme (Fig. 3 and Table 1).

A digital map of the geographical information system of the province Tyrol (Land Tirol, 2017) was used to locate the sampling plots according to the sampling scheme. In the field, the basic grid plots were first localized by means of a handheld GPS (model GPSmap 60CSx, Garmin International Inc., Olathe, KS, USA) with an accuracy of 1-8 meters. Further locations in between the basic grid plots were localized by means of a compass and a measuring tape. The identification of the exact coordinates was subsequently carried out by a high-precision receiver (model Leica Viva GS 25, Heerbrugg, Canton St. Gallen, Switzerland) and the real time kinematic technique (RTK) and subsequently converted from the ITRS2008 (GNSS) into the national coordinate system (Gauß-Krüger M28).

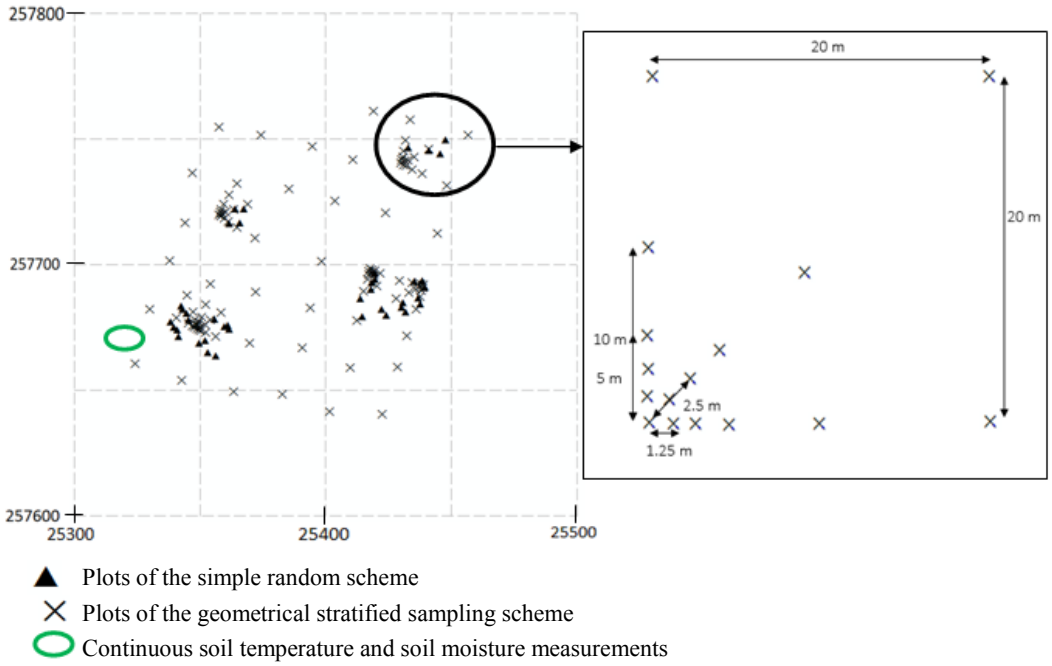

Fig. 3: Sampling scheme of the simple random plots (SRS) and the geometrical stratified sampling plots with different distance stages at the Reutte site.

2.3 Soil CO_2 efflux, heterotrophic respiration, autotrophic respiration and soil microclimate

Prior to the first measurement, each sampling location was equipped with PVC collars (diameter 10 cm, height 4 cm), inserted 3 cm into the soil and permanently fixed with tent pegs to avoid disturbance. Soil respiration was measured from the end of April to the end of October at the Hoellengebirge site and from mid-June to the end of October at the Reutte site. Soil CO_2 efflux was measured by means of a portable infrared gas analyzer (model EGM-4, PP Systems International, Inc., Amesbury, MA, USA) and an attached respiration chamber (model SRC-1, PP Systems International, Inc., MA, USA). The chamber was placed on top of each collar and the gas analyzer measured the change in the CO_2 concentration over a period of 124 seconds. If the increase was higher than 50 ppm per measurement interval (each 4.8 seconds), the measurement stopped. Simultaneously to the CO_2-flux measurements, the temperature at 5 cm (T_s) and 10 cm depth and soil moisture at 0 - 7 cm (VWC_s) depth were measured with a handheld thermometer and a calibrated soil moisture meter (model Field Scout TDR 100, Spectrum Technologies, Inc., IL, USA). To avoid perturbation, measurements were conducted at a 15-cm distance to the collars. Soil moisture measurements were repeated in a triangular pattern, to account for the heterogeneous soil and humus conditions. To avoid systematical sampling bias (especially due to diurnal variation in soil temperature), a randomized sequential arrangement of treatments and plots was alternated between the measurements. Continuous soil temperature and soil moisture measurements were made by means of 5 combined moisture - temperature sensors (model GS3, Decagon Devices, Inc., Pullman, WA, USA). Data were recorded in an hourly interval by means of a data logger (model EM50, Decagon Decives, Inc., Pullman, WA, USA). At the Hoellengebirge site, the GS3 sensors were installed close to the HU07 plots. At the Reutte site 3 sensors were installed at RU03 and 2 sensors at RF03.

To estimate the heterotrophic respiration and the contribution of autotrophic respiration (RaC) to R_s, 7 and 5 root exclusion plots with a dimension of 0.7 x 0.7 meters were installed at each treatment of the Hoellengebirge site and the Reutte site, except MS (Table 1). Because of limited resources an establishment of root exclusion plots was only possible in the UF and the FE, while in the MS at the Reutte site a RaC of 50% was assumed (Subke et al., 2006, Mayer et al., 2017b). The soil and the roots at the edges of these squares were excavated or cut down to the bedrock to attach a 3 mm pond foil. This should avoid the ingrowth of roots and

mycorrhizas. The above-ground biomass was removed. Therefore, the R_s rates of these root exclusion plots were considered as purely from R_h. In the rare occasions, when the R_h of the root exclusion plots was higher than R_s of the adjacent treatment, R_a was set to be zero. This phenomenon could be observed immediately after the establishment of the root exclusion plots. After correction for soil moisture and temperature the RaC was estimated by the subtraction of the average R_h of the root exclusion plots from the average R_s (separately for each treatment, see chapter 2.5.1).

Table 1: Distribution of the root exclusion plots, the number of plots for measuring R_s and the additional plots of the geometrical stratified sampling scheme for the locations and the treatments at the Hoellengebirge site and the Reutte site.

Site	Treatment	Root exclusion plots	Plots	Additional plots for spatial analysis
Hoellengebirge	HU07	yes	7	-
	HU07	no	23	-
	HF07	yes	7	-
	HF07	no	16	-
Reutte	RU03	yes	5	-
	RU03	no	16	35
	RF03	yes	5	-
	RF03	no	16	32
	MS	yes	-	-
	MS	no	8	38

2.4 Site parameters

Soil type, humus form, layer thickness [cm], soil depth [cm], soil cover [%], vegetation cover [%], canopy closure [%] and the dominant functional group were determined. Because of restricted resources, a site characterization at the Hoellengebirge site was not feasible. The classification of the specific soil types and their layer thickness at each measuring location was made by means of a soil corer (inner-diameter ~ 25 mm), which was hammered into the soil down to the bedrock. For this purpose, the corer was placed in a 50-cm distance to the collar (south directed). The classification was made in dependence on the *Austrian Soil Group Classification* (ASC) (Nestroy, 2011) and the *World Reference for Soil Resources* (WRB) (WRB, 2015)

The assessment of the humus forms was carried out by means of a spade (also in a 50-cm distance to the collars to avoid disturbance). The classification was made in dependence on the *Austrian Soil Group Classification* (ASC) (Nestroy, 2011) and the *European Humus Forms Reference Base* (EHFRB) (Zanella, 2011). Table 2 and Table 3 show the main characteristics of the identified soil types and humus forms at the research site at the Reutte site, respectively.

Table 2: Soil types of the research site at the Reutte site and their characteristics, classified according to the *Austrian Soil Classification* (ASC) and the *World Reference Base for Soil Resources* (WRB) (modified after Scheffer and Schachtschabel, 2016 and Nestroy et al., 2011).

ASC: **Fels-Auflagehumusboden**	WRB: **Folic Histosol** (if O > 10 cm) or **Lithic Leptosol** (if O < 10 cm)
Horizons: F-H-Cu; F-Cu • organic soil without any detectable fine-mineral components (sand, silt, clay) • distinctive H-layer (> L+F) above non-weathered parent material (relatively acid soil conditions) • pedogenesis is restricted by slightly degraded organic matter • minimal OC-content of 30 mass%	
ASC: **Rendzina**	WRB: **Rendzic Leptosol**
Horizons: Ahb-C; Ap-C; F-H-Ahb-Cv-Cn; F-H-C • organic, skeletal-rich soils above compact or loose calcareous rocks with more than 75 mass% $CaCO_3$ • A-horizon could be calcareous or non-calcareous, but in general base saturated • typical coloration is black to dark brown (calcium humates) • pedogenesis essentially based on the accumulation of humus • mineral components of the soil are fractions of the non-calcareous components of the parent material	
ASC: **Kalkbraunlehm-Rendzina**	WRB: **Rendzic cambic Leptosol**
Horizons: Ahb-AB-C; Ahb-BrelCv; F-H-AB-C; F-H-A-BrelC; A-B-C • soil type in transition between Rendzic Leptosol and Chromic Cambisol • calcareous parent material with more than 75 mass% of $CaCO_3$ • Ahb horizon with a stable, rich in humus and crumbly or polyhedral structure • clear color-differentiation between Ahb-horizon and calcareous-clay rich AB/ BrelC-horizons • maximum layer thickness of the B-horizon is 10 cm	
ASC: **Braunlehm**	WRB: **Chromic Cambisol**
Horizons: A-Bv,rel-C; A-Bv-C • mineral soil with an intensive yellow-brownish to red-brownish colored B-horizon with a blocky and sharp-edged structure and a loamy texture • parent material is calcareous with less than 25 mass% of non-calcareous components • relictic origin or long pedogenesis of the B horizon	

Table 3: Humus forms of the research site at the Reutte site and their characteristics classified according to the *Austrian Soil Classification* (ASC) and the *European Humus Forms Reference Base* (EHFRB) (modified after Nestroy et al., 2011).

ASC: **Mull**	EHFRB: **Mull**
• mainly 0-2 ecto-organic layers with absence of an H-layer • high biological activity which leads to a fast decomposition of the organic input and a crumbly structure in the A horizon • develops at locations with easily degradable foliage litter under balanced temperature and water conditions and $CaCO_3$ influence • oftentimes characterized by the presence of clay humus complexes	
ASC: **Moder**	EHFRB: **Moder**
• regularly 3 ecto-organic layers, while the L -layer < F+H • decomposition of organic matter mainly zoogenic and mycogenic or in combination of both • coprogenic components of arthrophods • An Ahb-horizon could be present but also replaced by an Ahi- or Ahe-horizon • can be found above all substrates, while the boundary between organic and mineral horizons is normally sharp (except for biological more active forms or forms influenced by grasses) • slower decomposition than on mull • can be found on all substrates	
ASC: **Alpenmoder**	EHFRB: **Tangel**
• sub-category of Moder humus with deep dark organic horizons up to a thickness of 20 cm (and more) • homogeneous with little coarse fraction and no mineral particles • very slow biodegradation (collembolas, anecic and endogeic earthworms) • on soils of the calcareous series	

The description of the microtopography (pit and mound, > ± 15 cm vertical difference to the surrounding area), percentage soil cover (rock, bare soil, debris and vegetation) and a subdivision of the vegetation in functional groups (moss, ligneous, shrubs (explicitly *Rubus sp.*), herbs & gras) was carried out for each sampling plot by means of a 50 x 50 cm metal frame (Kuuluvainen, 2003). To account for the adjacent trees, the most dominant tree species within a 1.5-m distance to the collars were noted. Also an estimation of the canopy cover of the collars was made by categories (high (>50%), medium (25-50%), low (5-25%), no canopy cover (<5%)) (Hotter, 2013).

Additional topographic parameters (elevation above sea level (m), slope gradient (%) and aspect (°)) were extracted from a digital elevation model (resolution: 1x1m) by using ArcMap (Environmental Systems Research Institute (Esri), Redlands, CA, USA). Each sampling plot was assigned to the specific treatment location.

2.5 Statistical analysis

Statistical data analysis and graphics were performed by the free software environment for statistical computing and graphics R v. 3.4.0 (R Development Core Team, 2016) using the package "nlme" (Pinheiro, 2000) and "ggplot2" (Wickham, 2009).

2.5.1 Calculation of soil CO_2 efflux, heterotrophic respiration, autotrophic respiration and soil microclimate

Descriptive statistics were computed for the measured R_s, T_s and VWC_s for the whole site and for the individual treatment, including mean value (mean), minimum (min) and maximum (max) values, standard deviation (SD), standard error of the mean (SE) and coefficient of variation (CV).

Effects of fencing on R_s as well as on T_s and VWC_s were tested by means of t-tests and analysis of variance (ANOVA) and subsequent Tukey´s HSD tests with mixed-effects model structure at a significance level of $p < 0.05$ (Pinheiro, 2000). Treatments and plots were assumed as fixed effects and random effects, respectively. Repeated measurements were nested within plots to account for the repeated measurement structure.

Soil temperature was the main factor controlling R_s during the observation period. Hence, a non-linear regression model was used to fit the relationship between R_s and the T_s data (Janssens and Pilegaard, 2003, Lloyd and Taylor, 1994):

$$R_s = \beta_1 e^{(\beta_2 T_s)} \quad \text{(Equ. 1)}$$

where R_s is the measured soil CO_2 efflux (μmol CO_2 m^{-2} s^{-1}) , T_s is the measured soil temperature (°C) at a soil depth of 5 cm and β_1 and β_2 are model coefficients.

The temperature sensitivity of the soil CO_2 efflux (the factor, by which R_s increases during a temperature rise of 10 °C) was calculated by means of the equation

$$Q_{10} = e^{\beta 10} \quad \text{(Equ. 2)}$$

where Q_{10} is the temperature sensitivity and β the particular β_2 model coefficient of equation 1.

The basal soil respiration at a soil temperature of 10 °C (R_{10}) was calculated by means of the equation

$$R_{10} = \beta_1 e^{(\beta_2 10)} \quad \text{(Equ. 3)}$$

where R_{10} is the basal soil respiration at 10 °C and β_1 and β_2 model coefficients of equation 1.

The relationship between R_s, Q_{10} and R_{10} can also be expressed as

$$R_s = R_{10}\, Q_{10}^{\left(\frac{T_S - 10}{10}\right)} \quad \text{(Equ. 4)}$$

where R_s is the soil respiration, R_{10} the basal soil respiration at 10 °C, Q_{10} the temperature sensitivity and T_s (°C) the measured soil temperature at a soil depth of 5 cm.

To prevent a potential bias between the two sites induced by the seasonal vegetation development, only measurements from the 18th of June until the 24th of October were included in the model.

The measured microclimatic parameters of the root exclusion plots differed markedly from the untreated plots, due to missing above-ground vegetation and therefore higher temperatures and lower water uptake by mycorrhizas and roots. To account for these microclimatic differences, a correction procedure was applied to CO_2 efflux measurements from root exclusion plots. In a first step, moisture corrections were performed according to Schindlbacher (2008) and Mayer et al. (2017b).

A moisture function developed by Mayer et al. (2017b) was used to predict CO_2 efflux under daily average VWC_s conditions of untreated plots and of root exclusion plots, respectively:

$$CO_2\ efflux = -0.11 + 0.02\ VWC_s - 0.0002\ VWC_s^2 \quad \text{(Equ. 5).}$$

The relative differences between the predicted fluxes were subsequently multiplied by the measured R_h rate. The corrections were conducted for each root exclusion plot and sampling date.

In a second step, moisture corrected R_h from the root exclusion plots were corrected for temperature by means of a transformation of equation 4. A widely accepted Q_{10} value of 2 was used to correct R_h to the daily average soil temperatures of the untreated plots following the protocol of Yuste et al. (2005).

As mentioned above, R_h at MS was assumed to account for 50% of the total soil respiration (Subke et al., 2006, Mayer et al., 2017b).

The relation between corrected R_h and soil temperature was fitted by equation 1. Seasonal temperature sensitivies and basal respiration at 10 °C were calculated by means of equation 2 and 3, respectively.

To ensure an adequate approach regarding the comparison of R_h and R_a between the two sites (caused by the different length of the observation period), they were also analyzed separately for the main foliation period from July until the end of September (Ellenberg, 1992).

The T_s and VWC_s were synchronized with the continuous measurements of the sensors to model plot specific respiration fluxes on a diurnal scale as well as for the whole measurement period. Therefore, mixed effects models (ME) were computed for each individual plot. Plots were used as random effects. Repeated measurements were nested within plots to account for the repeated measurement structure.

$$T_s = \beta_1 + \beta_2 T_{cont} + \beta_3 T_{cont}^2 \quad \text{(Equ. 6)}$$

where T_s is the measured soil temperature at 5 cm depth at the individual plot, β_1, β_2, β_3 are model coefficients and T_{cont} is the average measured soil temperature recorded by the data logger at the time of the measurement. A quadratic term was induced to account for potential shading effects. Homoscedasticity and normal distribution of the ME model were visually assessed by means of a QQ plot and a residual plot. The modeled T_s are in the following abbreviated as T_{model}.

The synchronization of the soil moisture was conducted by means of a linear ME model. Plots were used as random effects again. Repeated measurements were nested within plots to account for the repeated measurement structure.

$$VWC_s = \beta_1 + \beta_2 VWC_{cont} \quad \text{(Equ. 7)}$$

where VWC_s is the measured soil moisture, β_1 and β_2 are model coefficients and VWC_{cont} is the average measured soil moisture of the sensors at a specific time. Model diagnostics were also performed by a QQ plot and a residual plot. The modeled VWC_s are the following abbreviated as VWC_{model}.

R_s can also be restricted by too high or too low volumetric water content (Raich and Schlesinger, 1992, Mayer et al., 2014). Model comparisons based on minimal values of the Akaike Information Criterion (AIC) revealed significant better estimations with an inclusion of VWC_s as additional parameter. Therefore, to calculate R_s on a daily scale and also during the whole measurement period an exponential soil moisture term was added to equation 1 (Knohl et al., 2008). To linearize the relationship of R_s to T_s and VWC_s, R_s values were natural log-transformed prior to modeling.

$$Ln(Rs) = \beta_1 + \beta_2 T_s + \beta_3 VWC_s \quad \text{(Equ. 8)}$$

where Ln(Rs) is the natural log-transformed soil respiration, T_s is the soil temperature at 5 cm depth, VWC_s is the soil moisture and β_1, β_2 and β_3 are model coefficients. The modeled R_s are the following abbreviated as R_{model}.

To model the CO_2 efflux on a daily scale, the average treatment specific parameters of equation 8 were used in combination with the daily average measured T_{cont} and VWC_{cont} of the sensors and the average treatment specific parameters of equation 6 and 7.

A statistical comparison of the treatments regarding the modeled CO_2 efflux was not purposeful, due to the range of model insecurities and therefore high uncertainties of the estimates.

To estimate the total, the heterotrophic and the autotrophic soil CO_2 efflux over the whole measurement period, ME models were computed according to equation 8 for R_s of the untreated plots and the temperature and moisture corrected R_h of the root exclusion plots. Plots were used as random effects. Repeated measurements were nested within plots to account for the repeated measurement structure.

2.5.2 Site parameters controlling CO_2 efflux

Site parameter effects on R_s were only analyzed for Reutte site. The R_s rates were standardized for temperature at 10 °C (R_{10}) and for average treatment specific VWC_s prior to analysis. This was accomplished by the correction approach described in chapter 2.5.1. Only measurements of the last three measurement campaigns in 2016 were included to estimate R_{10}. The plots of the simple random scheme and the geometrical stratified sampling scheme (in total 145 plots) were used for the analysis. The average plot specific R_{10} rates and the assessed site parameters were used as dependent and independent variables for linear regressions, respectively. Two sample t-tests and ANOVA were used to analyze potential differences in R_{10} rates between factor variables (e.g. humus types). For the differentiation between factor levels, Tukey´s post-hoc tests were used. Two way ANOVA and analysis of covariance (ANCOVA) were used to account for interactions between treatments and site parameters with respect R_{10}. Level of significance was a $p < 0.05$.

2.5.3 Spatial correlation and mapping of CO_2 efflux

To explain spatial dependencies of R_s and to create maps to detect potential respiration hot spots, ordinary kriging was applied. All the established plots at the Reutte research site were used to quantify the spatial autocorrelation of R_s at different scales (Webster, 2001). The computation of the semivariograms and the ordinal kriging procedure were carried out by using ArcMap (version 10.4.1, ESRI, Redlands, CA, USA).

The premise of kriging, namely that plots closer to each other tend to be more similar than plots further apart, is called autocorrelation and is used to interpolate or predict unsampled plots in an area (Webster, 2001). Therefore, kriging is a common technique to analyze spatial

dependencies of variables. The basic tool in geostatistics is the classical variogram estimator based on (Matheron, 1963), which defines half the variance or semivariance γ(h) as follows:

$$\gamma(h) = \frac{1}{2\,N(h)} \sum_{i=1}^{N(h)} [z(x_i) - z(x_i + h)]^2 \quad \text{(Equ. 9)}$$

where γ(h) is the variance, N(h) is the number of data pairs at each specific separation distance h (also known as lag), $z(x_i)$ is the measured value at location x_i and $z(x_i + h)$ is the measured value at location $x_i + h$.

Applied to all data pairs of the data set, the variance can be plotted against the lag, resulting in an "experimental variogram" (Webster, 2001, Stoyan et al., 2000). Subsequently, the experimental variogram was fitted by an empirical variogram function, to interpolate soil CO_2 fluxes at unsampled locations. The empirical variogram is characterized by the nugget effect c_0, the partial sill c and the major range a. A nugget effect occurs if the semivariance at a lag distance of 0 m > 0. This can be explained by measurement errors or short-scale-variability over distances smaller than the shortest sampling interval. The major range is the distance between lag distance h = 0 and the lag distance at which the maximum variance is reached. This point is also called sill. The subtraction of the sill by means of the nugget effect reveals the partial sill, an indicator for spatial dependency. For the estimation of these parameters a spherical model was used according to the equation:

$$\gamma(h) = \begin{cases} c_0 + c\left[\frac{3h}{2a} - \frac{1}{2}\left(\frac{h}{a}\right)^3\right] & for\ h \le a, \\ c_0 + c & for\ h > a \end{cases} \quad \text{(Equ. 10)}$$

where γ(h) is the semivariance for a specific lag distance h, c_0 is the nugget effect, c is the partial sill and a is the major range value (Webster, 2001).

To analyze the magnitude of spatial dependence, a nugget coefficient n_c was calculated by means of the equation:

$$n_c = \frac{c_0}{c_0 + c} \quad \text{(Equ. 11)}$$

where c_0 is the nugget effect and c the partial sill. In case of $n_c < 0.25$ the variable is highly spatially correlated, if n_c varies between 0.25 and 0.75 it only shows a moderate spatial dependency and if $n_c > 0.75$, there is a small or no spatial dependence (Cambardella et al., 1994).

Measured R_s and T_s of both, the plots of the simple random scheme and the geometrical stratified sampling scheme were used for the geostatistical analysis. R_s fluxes were also log-transformed to account for the precondition of normal distribution of geostatistical analysis (Cressie and Hawkins, 1980).

3. Results

3.1 Effects of fencing on soil CO_2 efflux, heterotrophic respiration, autotrophic respiration and soil microclimate

The measured R_s clearly followed the seasonal pattern of T_s (Fig. 4 and Table A1 - A3 in the appendix). Therefore, maximum R_s was detected at the maximum T_s for both sites. Average R_s was 3.21 and 3.68 µmol CO_2 m^{-2} s^{-1} at HU07 and HF07 and 6.66, 4.95 and 4.19 µmol CO_2 m^{-2} s^{-1} at RU03, RF03 and MS, respectively. The coefficient of variation (CV) as a measure of spatial variation ranged between 39 and 59% at the Hoellengebirge site and between 38 and 63% at the Reutte site. No temporal pattern of CV regarding R_s could be detected at the Hoellengebirge site nor the Reutte site, except for MS where an increasing trend was observed. No significant treatment effects on Rs were determined at the Hoellengebirge site (Table A4). At the Reutte site, no significant differences in R_s were determined for RF03 and MS, but significantly higher Rs rates were determined for RU03 (Table A4).

Soil temperature showed typical seasonal patterns at both sites, with maximum values in late July with 21.06 and 18.89°C at HU07 and HF07 and 19.72, 16.58 and 17.09°C at RU03, RF03 and MS, respectively (Fig. 4b and e). Average T_s over the whole measurement period was 15.4 and 15.0°C at HU07 and HF07 and 15.5, 13.6 and 12.9°C in the RU03, RF03 and MS at the Reutte site, respectively. The unfenced treatments showed continuously higher temperatures than the fenced treatments, except at the first measurement (Hoellengebirge site) and the measurement campaign at the end of October (both sites), where T_s in the fenced treatments at both sites was higher than in the unfenced treatments. CV increased with decreasing temperature. T_s during the complete measurement season was not significantly different between the treatments at the Hoellengebirge, but significantly different at the Reutte site between RU03 and both RF03 and MS ($p < 0.05$) (Table A4). Within the foliation intensive period from mid June to the end of September, significant temperature differences between the treatments could also be detected at the Hoellengebirge site ($p < 0.05$).

VWC_s was nearly stable between 30-40% at both sites, with an average of 36.0 and 33.3% at HU07 and HF07 and 34.3, 36.4 and 33.7% in RU03, RF03 and MS at the Reutte site, respectively (Fig. 4 c & f). At the Hoellengebirge significant differences could be detected with respect to VWC_s, while the treatments did not differ significantly ($p < 0.05$) at the Reutte site (Table A4).

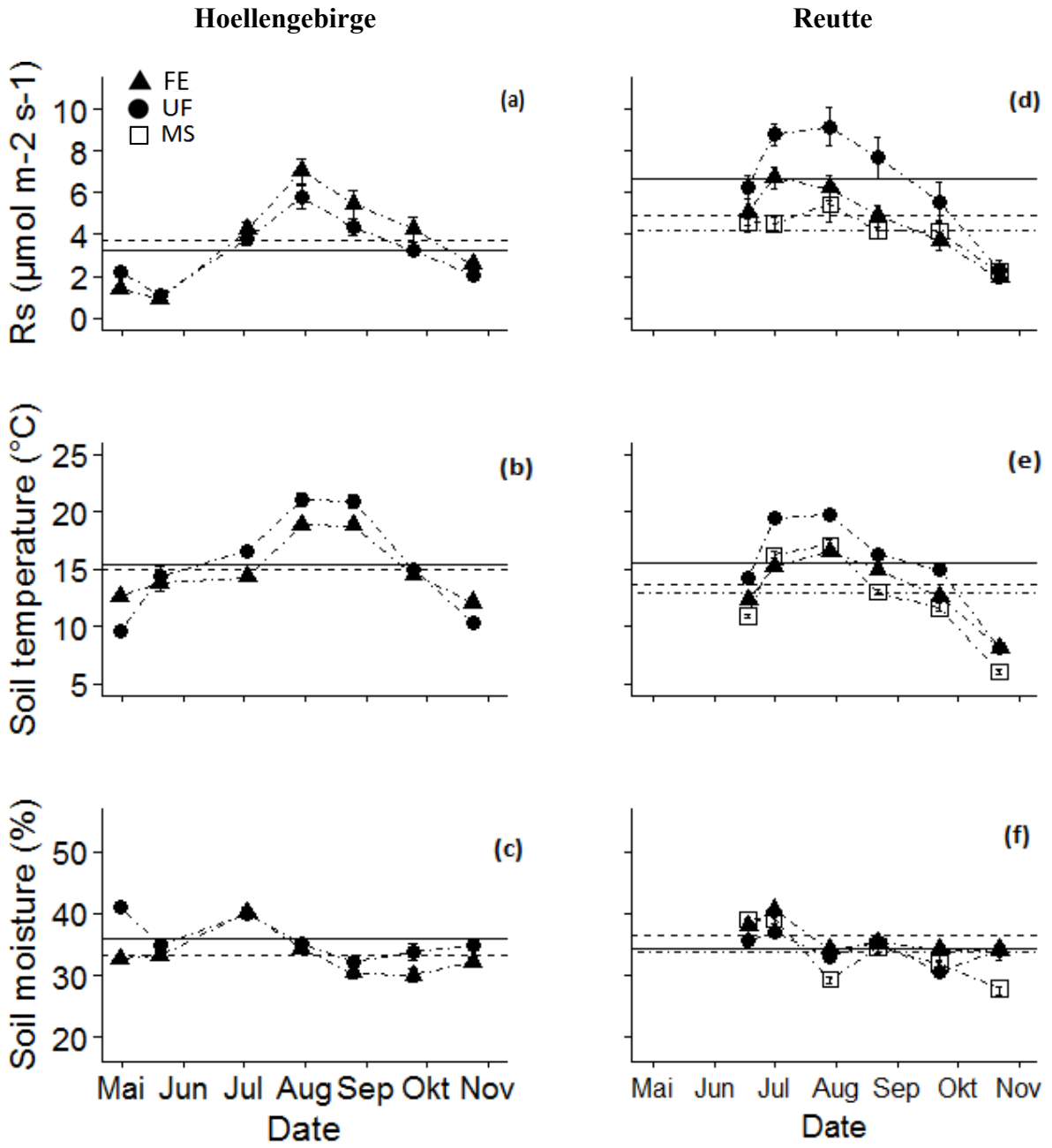

Fig. 4 : Comparison of the Hoellengebirge site (a-c) and at the Reutte site (d-e) regarding average (mean +/- SE) CO_2 efflux (R_s) (a & d), soil temperature (b & f) and soil moisture (c & f) of the unfenced treatment (UF), the fenced treatment (FE) and the mature stand (MS) during the measurement period from May until end of October. Horizontal lines indicate the average of the respective variable during the measurement period (solid line = UF, dotted line = FE, dotdashed line = MS).

The temporal patterns of R_h and R_a were similar to those of R_s (Fig. 4 a & d and Fig.5 a, b, d &e). Average R_h and R_a at the Hoellengebirge site during the whole measurement period was 2.13 and 1.09 µmol CO_2 m^{-2} s^{-1} at HU07 and 2.34 and 1.34 µmol CO_2 m^{-2} s^{-1} at HF07, respectively. R_h was not significantly different between HU07 and HF07 during the whole observation period nor for the main foliation period (Table A5). Autotrophic respiration

between the treatments at the Hoellengebirge site differed only marginal significantly ($p = 0.083$) during the whole observation period. Significant higher R_a rates ($p < 0.05$) could be detected in HF07 during the phase of foliation from end of June until end of September when compared to HU07 (Table A5).

At the Hoellengebirge site maximum R_h and R_a was 3.47 ± 0.29 µmol CO_2 m^{-2} s^{-1} and 3.55 ± 0.29 µmol CO_2 m^{-2} s^{-1} (percentage of autotrophic respiration on the total soil respiration (RaC) = 51%) at HF07 at the 30th of July 2016, respectively. Also at the same campaign HU07 showed the highest R_h and R_a fluxes with 3.34 ± 0.30 µmol CO_2 m^{-2} s^{-1} and 2.46 ± 0.22 µmol CO_2 m^{-2} s^{-1} (RaC = 42%), respectively (Fig. 5a-c). During the whole measurement period average RaC was 33 and 28% at HU07 and HF07, respectively. In the phase of foliation from July until the end of September, RaC was 34 and 40% at HU07 and HF07, respectively. The highest RaC at HU07 and HF07 could be detected at the end of October (RaC = 46%) and at the end of July (RaC = 51%), respectively.

Average measured R_h and R_a at the Reutte site was 4.71 and 1.95 µmol CO_2 m^{-2} s^{-1} at RU03 and 3.43 and 1.52 µmol CO_2 m^{-2} s^{-1} at RF03, respectively (Fig. 5d & e). A supposed heterotrophic contribution of 50% revealed an average R_h of 2.1 µmol CO_2 m^{-2} s^{-1} at MS. During the whole measurement period as well as during foliation intensive period heterotrophic respiration was significantly higher at RU03 when compared to RF03 and MS ($p < 0.05$) (Table A5). R_h of RU03 was significant higher when compared to MS at the foliation intensive period, while no significant differences between these treatments were detected during the whole measurement period nor for R_a. Autotrophic respiration was significantly higher at RU03 than at RF03 during the foliation intensive period ($p < 0.05$), but not during the whole measurement period (Table A5).

At the Reutte site, maximum R_h and R_a was 6.27 ± 0.53 µmol CO_2 m^{-2} s^{-1} and 3.54 ± 0.35 µmol CO_2 m^{-2} s^{-1} (RaC = 39%), measured at the RU07 at the first campaign (18.06.2016) and the third campaign (29.07.2016), respectively (Fig. 5 d-f). Maximum R_h and R_a at the RF03 was 5.06 ± 0.91 µmol CO_2 m^{-2} s^{-1} and 2.29 ± 0.20 µmol CO_2 m^{-2} s^{-1} (RaC = 34%) at the first measurement campaign (18.06.2016) and at the second measurement campaign (01.07.2016), respectively. At MS, maximum R_h and R_a was 2.73 µmol CO_2 m^{-2} s^{-1} at the third campaign (29.07.2016). The average RaC at the RU03 and RF03 was at each treatment 29% during the whole measurement period from mid June until end of October and 33 and 34% during the phase of foliation, respectively. The highest RaC at RU03 and RF03 could be detected in the end of October (RaC = 45%) and September (RaC = 41%), respectively (Fig. 5f).

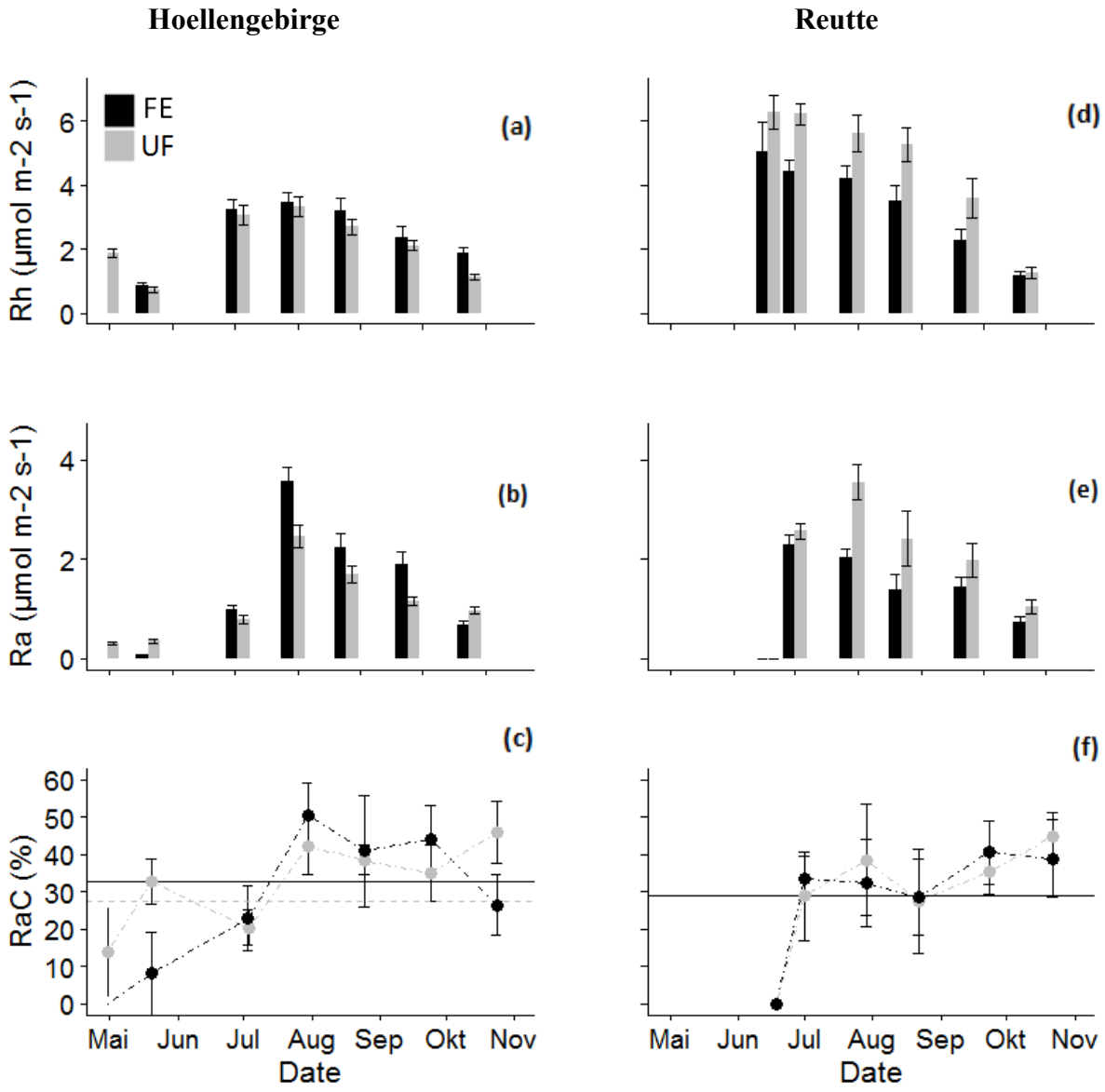

Fig. 5: Seasonal variations of (a) & (d) soil heterotrophic respiration (R_h), (b) & (e) soil autotrophic respiration rates (R_a) and (c) & (f) the contribution of autotrophic respiration to the total respiration (RaC) at the Hoellengebirge site and at the Reutte site, respectively. The data reflect the average values (mean ± SE) of each measurement campaign between the period from end of April to end of October 2016. In cases when R_h were higher than R_s, R_a was set to be zero.

Both R_s and R_h were strongly related to T_s (R^2 between 0.85-0.93 for R_s and 0.61-0.93 for R_h, Fig. 6 and Table 4). The fenced treatments at the Hoellengebirge site and at the Reutte site had 1.34 and 1.26 times higher Q_{10} values for R_s than the unfenced treatments, respectively. While the R_{10} at the younger windthrow at HF07 was higher when compared to HU07 (2.45 vs. 2.17 µmol CO_2 m^{-2} s^{-1}, respectively), the Reutte site revealed the opposite (3.08 vs. 3.74 µmol CO_2 m^2 s^{-1} at RF03 and HU07, respectively).

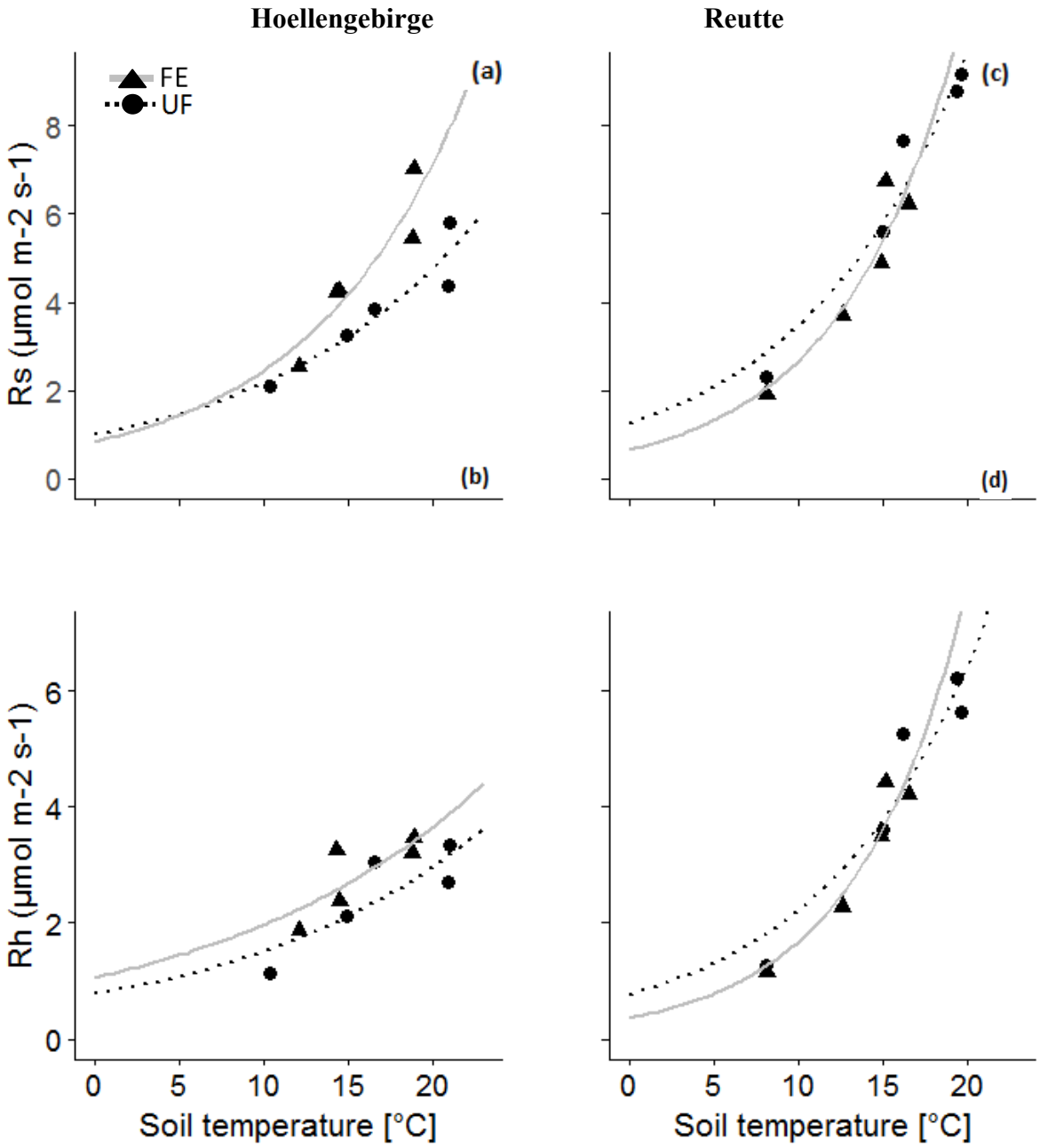

Fig. 6: Total soil respiration (R_s) (a&c) and heterotrophic respiration (R_h) (b&d) in dependence to soil temperature during the measurement period from mid June to end of October, separated by Treatment (dotted = UF, solidline = FE) for the research sites at the Hoellengebirge site (a & b) and at the Reutte site (c & d). Regression lines were fitted by means of euqation 1 ($R_s = \beta_1 e^{(\beta_2 T_s)}$).

Table 4: Summary of the treatment specific regression model of soil respiration after equation 1 ($R_s = \beta_1 e^{(\beta_2 T_s)}$) in respect to soil temperature, where R_s is the CO_2-efflux (µmol CO_2 m^{-2} s^{-1}) and T_s is the soil temperature (°C). Q_{10} is the temperature sensitivity calculated by means of equation 2 ($Q_{10} = e^{\beta 10}$) and R_{10} is the basal soil respiration at 10 °C calculated by means of equation 3 ($R_{10} = \beta_1 e^{(\beta_2 10)}$).

Location	Treatment	Respiration	β_1			β_2			Q_{10}	R_{10}	R^2
Hoellengebirge	HU07	R_s	0.994	±	0.387	0.078	±	0.02	2.2	2.2	0.85
	HU07	R_h	0.773	±	0.427	0.067	±	0.03	2.0	1.5	0.93
	HF07	R_s	0.842	±	0.411	0.107	±	0.03	2.9	2.5	0.91
	HF07	R_h	1.059	±	0.512	0.062	±	0.03	1.9	2.0	0.91
Reutte	RU03	R_s	1.449	±	0.422	0.095	±	0.02	2.6	3.7	0.93
	RU03	R_h	1.38	±	0.399	0.077	±	0.04	2.2	3.0	0.66
	RF03	R_s	0.949	±	0.524	0.118	±	0.04	3.3	3.1	0.85
	RF03	R_h	0.946	±	0.037	0.095	±	0.04	2.6	2.5	0.61

The mixed effect model to predict R_s (Equ. 8) in dependence to T_{model} (Equ. 6) and VWC_{model} (Equ. 7) explained 84% (RMSE of 1.27 µmol CO_2 m^{-2} s^{-1}) and 86% (RMSE of 1.26 µmol CO_2 m^{-2} s^{-1}) of the variance at the Hoellengebirge site and the Reutte site, respectively (Table 5). Normal distribution and homoscedasticity was found for the models at both sites (Fig. A1). ME models to predict R_s without VWC_s as an additional covariate revealed an R^2 of 0.79 at both sites.

Table 5: Summary of the plot specific mixed effect model of soil respiration after equation 8 ($Ln(Rs) = \beta_1 + \beta_2 T_s + \beta_3 VWC_s$) in dependence to soil temperature and soil moisture where R_s is the CO_2 efflux (µmol CO_2 m^{-2} s^{-1}), β_1, β_2 and β_3 model coefficients, Ts the soil temperature (°C) and VWC_s the volumetric water (%) content.

Location	Treatment	β1	β2	β3	R^2
Hoellengebirge	Site	-0.487 ± 0.066	0.082 ± 0.003	0.013 ± 0.002	0.84
	HF07	-0.347 ± 0.086	0.076 ± 0.003	0.008 ± 0.002	0.83
	RF07	-0.689 ± 0.081	0.091 ± 0.003	0.019 ± 0.002	0.82
Reutte	Site	-1.065 ± 0.174	0.121 ± 0.004	0.025 ± 0.003	0.86
	RU03	-1.108 ± 0.290	0.123 ± 0.007	0.027 ± 0.004	0.85
	RF03	-1.500 ± 0.216	0.132 ± 0.005	0.032 ± 0.004	0.85
	MS	-0.110 ± 0.310	0.094 ± 0.007	0.008 ± 0.005	0.89

The function to fit T_{model} (Equ. 6) explained 93% (RMSE of ±1.07 °C) and 89% (RMSE of ±1.27 °C) of the temporal variation in T_{model} at the Hoellengebirge site and at the Reutte site, respectively. Residuals were normal distributed and homoscedastic (Fig. A2).

As mentioned above, an inclusion of VWC_s as an additional parameter in to model R_s (Equ. 8) led to significant better estimates. The model to fit VWC_s (Equ. 7) explained 75% (RMSE of ±2.4 %) and 71% (RMSE of ±2.4 %) of the variation in VWC_{model} at the Hoellengebirge site and at the Reutte site, respectively. Residuals were normal distributed and homoscedastic (Fig. A3).

Tables A6-A8 in the appendix show the modeled CO_2 efflux (Equ. 8), the modeled temperature at a depth of 5 cm (Equ. 6) and the soil moisture (Equ. 7) for each measurement campaign for the complete site and the different treatments. As mentioned above, to avoid a bias in the models induced by the vegetation development, only measurements between mid-June and the end of October were included in calculating the models. Therefore, the modeled estimates of the first and second campaign at the Hoellengebirge were put in brackets.

Figure 10 reflects the R_{model}, T_{model} and VWC_{model} during the whole measurement period (mid of July until end of October).

At the Hoellengebirge site T_{model} and VWC_{model} showed an average of 13.4 °C and 14.9 °C and 35.1 % and 33.8 % at HU07 and HF07, respectively (fig. 7 b & c). At the Reutte site the mean T_{model} and VWC_{model} was 14.9 °C, 12.7 °C and 12.8 °C and 33.4 %, 35 % and 32 % at RU03, RF03 and MS, respectively (fig. 10 e & f). T_{model} and VWC_{model} differed between the treatments, except T_{model} between RF03 and MS. While VWC_{model} oscillated between 20 - 40% at the Hoellengebirge site - indicating drought periods in middle and the end of September - VWC_{model} at the Reutte site was relatively stable.

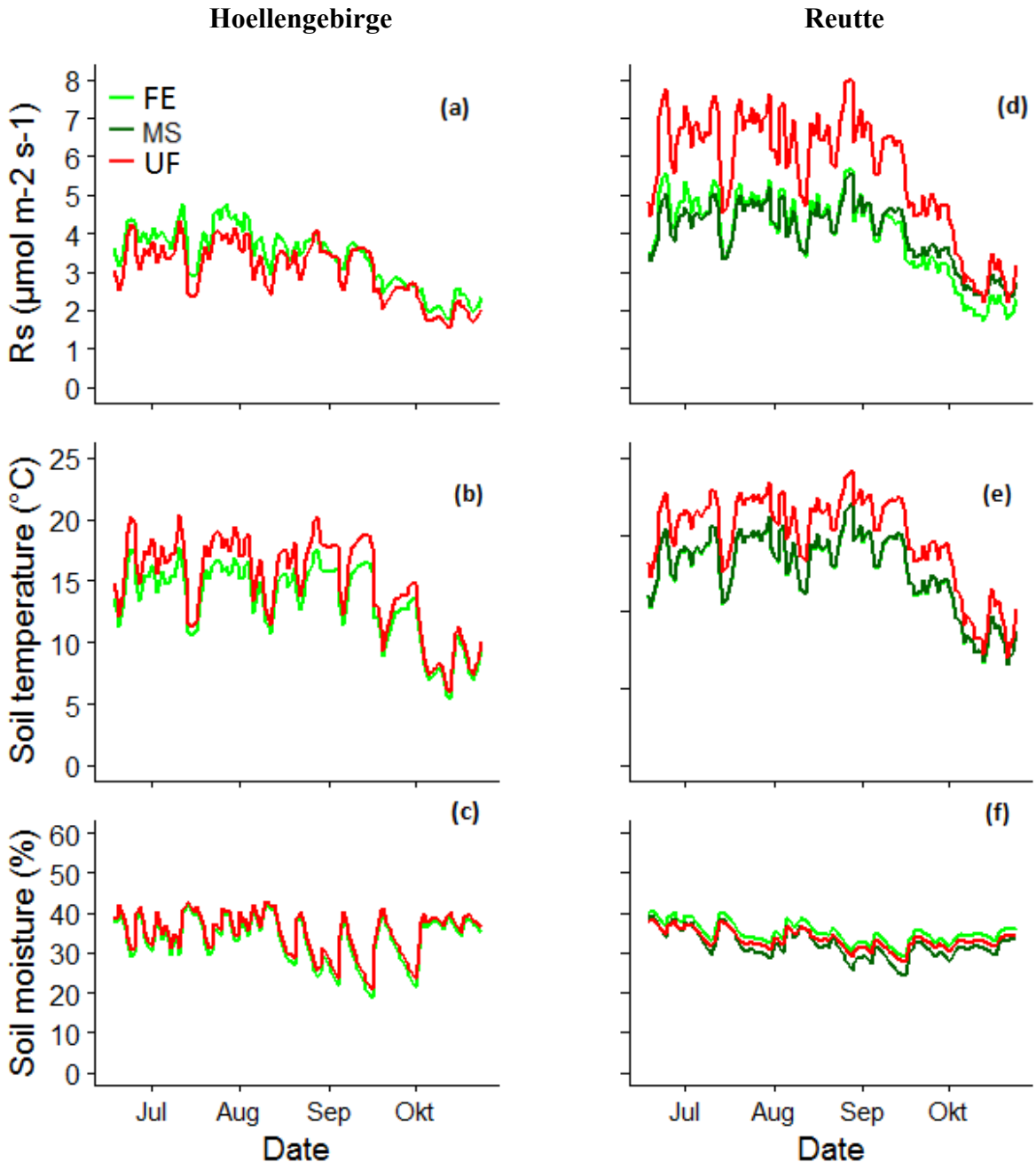

Fig. 7: R_{model} (a & d), T_{model} (b & e) and VWC_{model} (c & f) after equation 6-8 over the measurement period from mid 18.06.2016 until 24.10.2016 for the fenced (green), unfenced (red) and the mature stand (dark green) treatment at the Hoellengebirge site and at Reutte site.

Regarding the average sum of the C efflux during the measurement period, the treatments between the sites showed different patterns (Fig. 8 and Table A9). While at the younger windthrow the highest C efflux could be detected at HF07 (460 ± 38 gC m^{-2}), the older windthrow revealed the highest C efflux at RU03 (727 ± 58 gC m^{-2}). The mean C efflux of R_h in the HU07 and HF07 during the measurement period from 18.06.2016 - 24.10.2016 was 255 ± 17 and 299 ± 26 gC m^{-2} and 498 ± 31 and 328 ± 27 gC m^{-2} at RU03 and RF03, respectively. Surprisingly, the contribution of R_a to the total respiration was nearly at the same level of 37 and 35% for HU07 and HF07 and 32 and 35% for RU03 and RF03.

In the MS at the Reutte site R_s during the whole measurement period was 521 ± 55 gC m^{-2} and therefore comparable with the fenced treatment (501 ± 43 gC m^{-2}) (Fig. 8, Table A9). A supposed heterotrophic contribution of 50% revealed a heterotrophic efflux of 264 gC m^{-2} which is by far lower than the R_h at RU03 (498 gC m^{-2}).

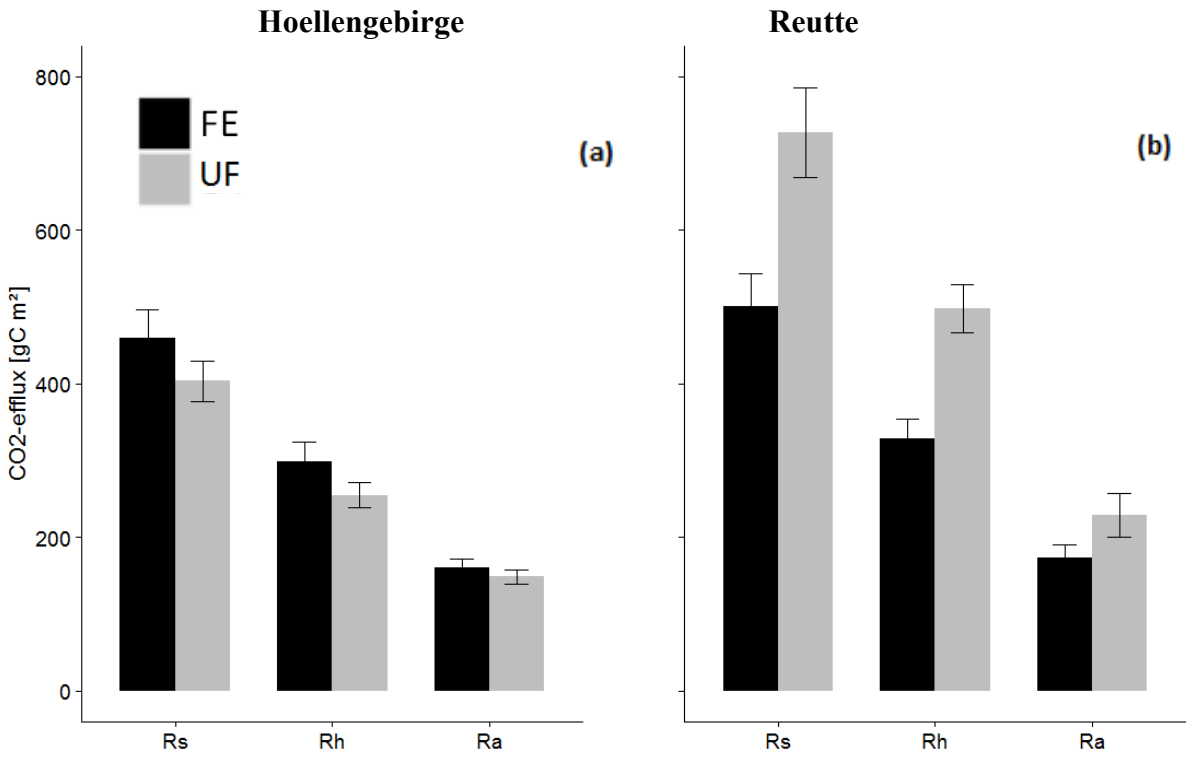

Fig. 8: Comparison of the modeled amount of emitted C during the measurement period from 18.06.2016 to 24.10.2016 in the unfenced (UF) and the fenced (FE) treatment at the Hoellengebirge site (a) and at the Reutte site (b).R_s, R_h and R_a represent the total soil respiration, heterotrophic and autotrophic respiration, respectively. R_a was calculated by the subtraction of R_s by R_h. Error bars represent the standard error of the mean.

3.2 Site parameters controlling CO_2 efflux

Significant influence on R_{10} could be detected for the factor variables "Soil group", "Humusform" and "Microtopography" as well as for the variables "Slope (°)", "Soil depth (cm)", "O-horizon (cm)", "OA-horizon (cm)", "A-horizon (cm)", "B-horizon (cm)", "Vegetation cover (%)", "Grass (%)" and "Bare soil cover (%)" and the interactions of "Slope x Treatment", "O-horizon x Treatment", "Debris cover x Treatment" (Table 6). The R_{10} was significantly higher at RU03 when compared to RF03, while no differences could be detected for MS and RU03 as well as RF03 (Fig. 9a, Table A10a). In general, plots on accumulation locations with mineral horizons (Rendzic cambic Leptosol and Chromic Cambisols) at lower slopes and elevations emitted more CO_2 at a soil temperature of 10 °C than plots with organic soils (folic Histosols and rendzic Leptosols) at mounds on higher slopes and elevations (Fig. 9b, Table 7, Table A10). Mull humus showed higher R_{10} values than Moder and Tangel (Fig. 9c, Table A10c), despite the fact that significant differences could only found between the humus forms Mull and Moder. The thickness of the O-horizon (cm) influenced the R_{10} negatively, while the thickness of the OA-horizon, A-horizon and B-horizon (cm) correlated positively with $R_{10.}$ Also the percentage of vegetation cover and explicitly grass cover influenced the R_{10} positively, while the percentage of bare soil showed a negative effect on R_{10}. Also the interaction between the treatments and the site parameters slope (°), layer depth of the O-horizon (cm) and debris cover (%) turned out to have significant influence on R_{10}. The negative correlation between the interaction of slope (°) and treatments with respect to R_{10} was more pronounced at RF03 and MS. The interaction between the thickness of O-horizon (cm) and the treatments revealed a negative effect at RU03, while at RF03 and MS no significant correlation could be detected. The effect of debris cover was only significant at RU03 and showed a negative correlation. Overall, the fenced treatments and MS showed closer similarities regarding the influence of continuous parameters compared to RU03 (Table 6).

Table 7 shows different site parameters of each treatment. RU03 and RF03 showed a relatively high proportion of mineral soils and the humus form of Mull, whereby MS was dominated by organic soils and a Moder humus form. Also, the layer depths are reflecting the humus forms and soil types: RU03 and RF03 show very similar depths of the O- and A-horizon with an average layer depth of 2.4 and 3.7 cm and 16.0 and 17.6 cm, respectively. MS show deep humus layers with a mean depth of 8.8 cm and relatively shallow A-layers with an average depth of 6 cm. The same could be observed regarding soil depth, resulting in deeper

soils in the RF03 (mean 33.0 cm) and RU03 (mean 25.2 cm) and relatively shallow soils in MS (mean 15.9 cm). The mean slope was 28.7, 28.6 and 29.5° at RU03, RF03 and MS, respectively. The mean elevation was approximately similar at around 950 meters a.s.l.. RU03 exhibited the highest vegetation cover of around 95%, followed by the RF03 and MS with 88 and 69%. At all treatments, grass was the most dominating vegetation form 0 - 30 cm above surface. The canopy closure at MS and RF03 was much higher when compared to RU03. Coniferous and deciduous trees dominated at MS and RF03, while at RU03 showed a superior proportion of grass cover.

The effect of the vegetation variables "canopy cover" and "functional group" on the measured T_s was also considered in the analysis. The plots with "high" and "medium" canopy closure showed significant lower temperatures when compared to plots with "no canopy cover". Additionally, the functional vegetation group "conifers" as well as "deciduous" showed significantly higher R_s when compared to "grass" during the observations period ($p < 0.05$).

Table 6: Summaries of two sample t-tests and ANOVA comparing R_{10} in relation to different factor variables and summary statistics of a linear models describing the relationship of R_{10} to different site and topographic variables and statistical summaries of two way ANOVA and ANCOVA and linear models to account for interactions between treatments and site parameters with respect to R_{10}. Significant correlations are pointed out by bolded p-values ($p < 0.05$).

	DF	slope coefficient	p-value	R^2		interaction with treatment				
						slope coefficient				
					DF	RU03	RF03	MS	p-value	R^2
factor variables										
Treatment	2	-	0.060	-		-	-	-	-	
Soil group	1	-	**0.001**	0.11	2	-	-	-	0.130	-
Humusform	2	-	**0.049**	0.03	4	-	-	-	0.933	-
Microtopography	1	-	**0.001**	0.19	2	-	-	-	0.092	-
canopy cover	3	-	0.061	-	6	-	-	-	0.341	-
functional group	5	-	0.147	-	10	-	-	-	0.310	-
continuous variables										
Slope (°)	1	-0.035	**0.003**	0.05	2	-0.007	-0.057	-0.083	**0.008**	0.13
Aspect (°)	1	-0.004	0.203	-	2	-0.012	0.017	0.017	0.091	-
Soil depth (cm)	1	0.021	**0.003**	0.05	2	0.045	-0.028	-0.014	0.213	-
O-horizon (cm)	1	-0.043	**0.049**	0.02	2	-0.607	0.552	0.595	**0.001**	0.13
OA-horizon (cm)	1	0.029	**0.033**	0.02	2	0.061	-0.041	-0.033	0.447	-
A-horizon (cm)	1	0.032	**0.006**	0.04	2	0.075	-0.032	-0.049	0.277	-
B-horizon (cm)	1	0.029	**0.005**	0.05	2	0.068	-0.046	-0.016	0.087	-
Vegetation cover (%)	1	0.017	**0.002**	0.06	2	0.045	-0.029	-0.030	0.233	-
Moss (%)	1	-0.008	0.084	-	2	-0.020	0.022	0.013	0.125	-
Ligneous (%)	1	0.008	0.835	-	2	0.122	-0.062	-0.175	0.319	-
Shrubs (%)	1	0.002	0.863	-	2	-0.013	0.018	0.061	0.169	-
Rubus (%)	1	0.008	0.403	-	2	0.041	-0.039	-0.036	0.370	-
Herbs (%)	1	0.022	0.440	-	2	0.029	-0.027	0.052	0.284	-
Gras (%)	1	0.013	**0.005**	0.05	2	0.018	-0.015	-0.009	0.355	-
Rock cover (%)	1	-0.035	0.055	-	2	-0.117	0.096	0.093	0.263	-
Debris cover (%)	1	-0.009	0.406	-	2	-0.080	0.077	0.086	**0.035**	0.06
Bare soil cover (%)	1	-0.020	**0.006**	0.04	2	-0.028	-0.002	0.009	0.849	-

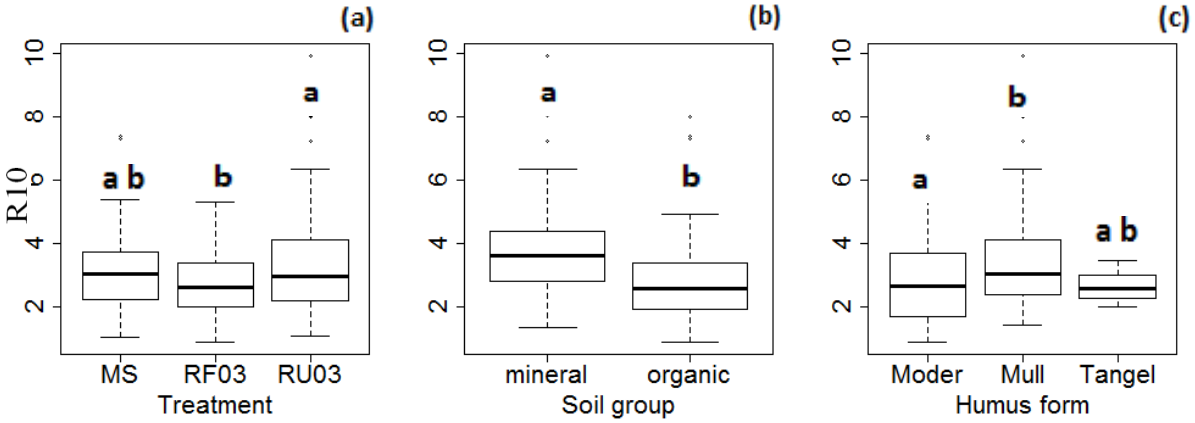

Fig. 9: Box and whisker plots of R_{10} depending on the variables "treatment", "soil group" and "humus form". Different letters indicate significant differences between factors levels on a site scale ($p < 0.05$).

Table 7: Characterization of each treatment with respect to the assessed site parameters. Represented are the identified numbers of each humus form, soil type, soil group and microtopography and also the averages of layer depths of soil horizons (cm), soil cover (%), vegetation cover (%), canopy closure (%), functional groups (%), slope (°), aspect (°) and elevation a.s.l. (m).

	Treatment			
	RU03	RF03	MS	
Humusform				Σ
Tangel	-	1	2	3
Moder	10	12	43	65
Mull	41	35	1	77
Σ	51	48	46	145
Soiltype				
Folic Histosols	2	1	29	32
Rendzic Leptosol	29	22	12	63
Rendzic cambic Leptosol	8	4	5	17
Chromic Cambisol	12	21	-	33
Σ	51	48	46	145
Soil cover (%)				
Rock	1	3	4	
Bare	1	4	14	
Debris	3	5	13	
Vegetation	95	88	69	
Σ	100	100	100	
Canopy closure				
no canopy cover (< 5%)	82	4	0	
low (0-25 %)	10	0	0	
medium (25-50%)	4	10	17	
high (< 50%)	4	85	83	
Σ	100	100	100	
Parameter				
Slope (°)	28.7 ± 2.0	28.6 ± 1.2	29.5 ± 1.3	
Aspect (°)	100.5 ± 5.6	109.2 ± 4.4	72.1 ± 3.7	
Elevation (m)	948.7 ± 3.4	943.9 ± 2.5	943.7 ± 3.3	

	Treatment			
	RU03	RF03	MS	
Layer depth (cm)				
O	2.4 ± 0.2	3.6 ± 0.8	8.8 ± 0.7	
A/Ah/AC	16.0± 1.2	17.6 ± 1.3	6.0 ± 1.5	
AB/BC/B	6.8 ± 1.6	12.7 ± 2.2	1.2 ± 0.6	
Σ	25.2± 2.4	34 ± 2.8	15.9 ± 1.7	
Soil group				Σ
Organic	31	23	41	95
Mineral	20	25	5	50
Σ	51	48	46	145
Vegetation cover 0-30 cm above surface (%)				
Moss	33	23	20	
Ligneous	0	1	1	
Shrubs	3	5	2	
Rubus	4	8	4	
Herbs	10	13	8	
Grass	45	38	34	
Σ	95	88	69	
Functional group (%)				
coniferous	8	31	98	
decidious	0	48	0	
grass	63	8	2	
herbs	6	2	0	
moss	14	4	0	
shrubs	10	6	0	
Σ	100	100	100	
Microtopography				Σ
Pit	28	25	26	79
Mound	23	23	20	66
Σ	51	48	46	145

3.3 Spatial correlation and mapping of CO_2 efflux

Spatial correlation of R_s ranged from 18.1 to 28.9 meters, while a successive decline with decreasing temperatures could be observed (Fig. 10-13, Table 8). The nugget coefficient ranged between 0.42 and 0.53, indicating only moderate spatial dependency, while the measurement campaign with the highest temperatures revealed the highest spatial autocorrelation. The general high nugget effect indicates a high spatial heterogeneity which was not covered by the sampling scheme. However, figures 11 - 13 reflect the interpolated T_s and R_s for each measurement campaign for the whole site. The visual assessment shows higher CO_2 fluxes in the unfenced treatment than in the other treatments, especially at the measurement campaign in August. In general, the areas identified as "hot spots" show the same behavior on every map.

Table 8: Variogram summaries for the measurement campaigns 4, 5 & 6, which include the plots of the SRS and the geometrical stratified scheme. Spatial correlations of R_s were modeled by means of a spherical model.

RecNo - Date	Mean Rs	Model	Partial sill	Range (m)	Nugget coefficient
4 - 22./ 23.08.2016	5.49	Nugget Spherical	0.113 0.157	0 28.9	0.42
5 - 22./ 23.09.2016	4.32	Nugget Spherical	0.121 0.108	0 22.6	0.53
6 - 21./22.10.2016	2.14	Nugget Spherical	0.133 0.130	0 18.1	0.51

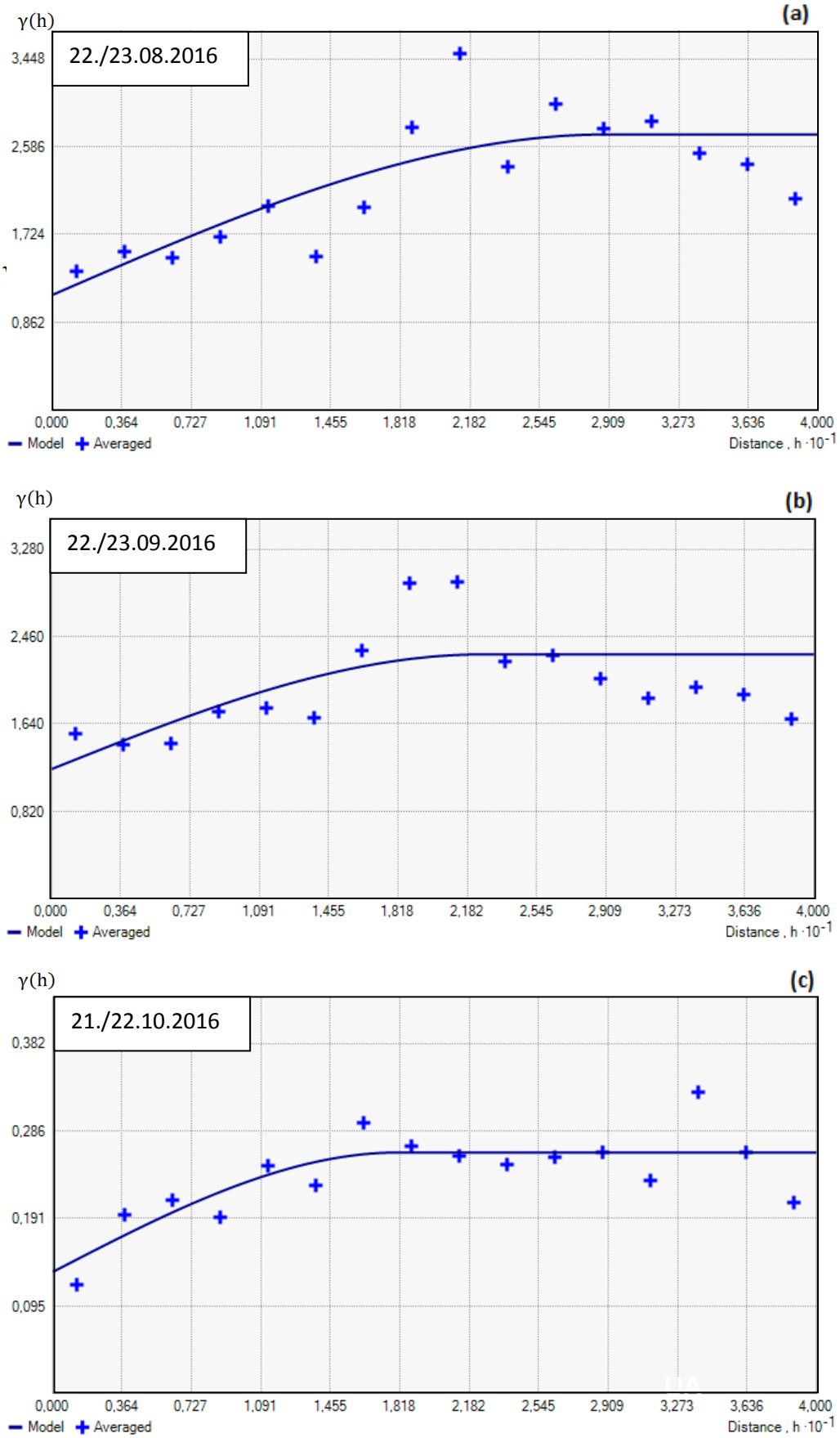

Fig. 10: Variograms of R_s for the measurement campaigns (a-c) including the plots of the simple random scheme and the geometrical stratified sampling scheme. Spatial correlation of the measured R_s were modeled by means of a spherical model.

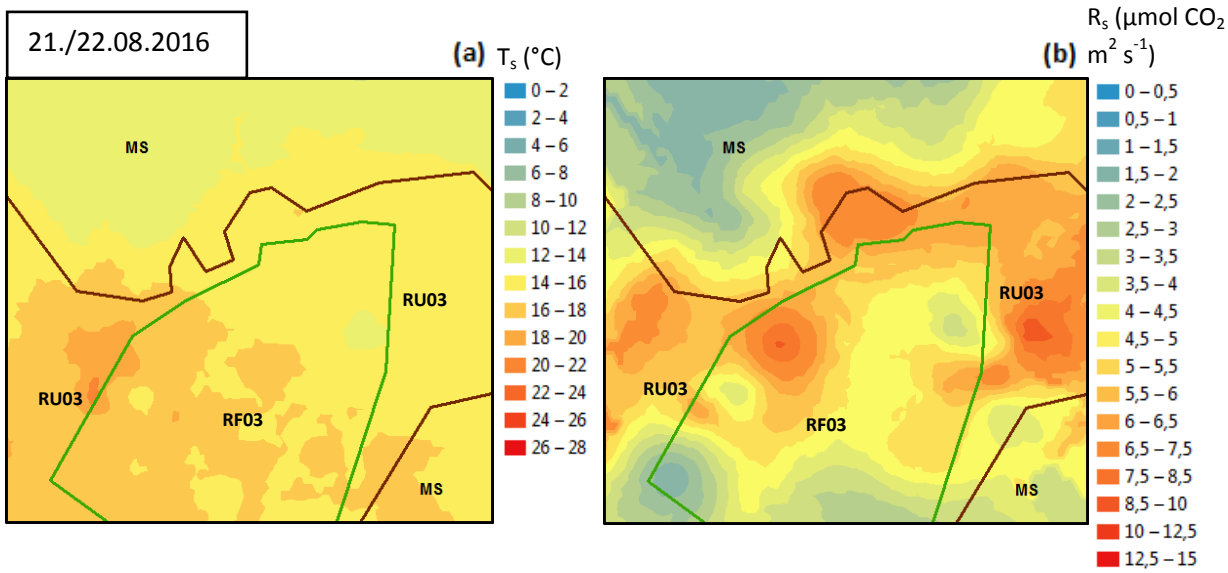

Fig. 11: Ordinal kriging map for the measured and interpolated soil temperature (T_s) (a) and soil respiration (R_s) (b) for the fourth measurement campaign at the 22./23.08.2016. The green line indicates the fenced treatment (RF03), the brown line the mature stand (MS) and the in-between area the unfenced treatment (RU03).

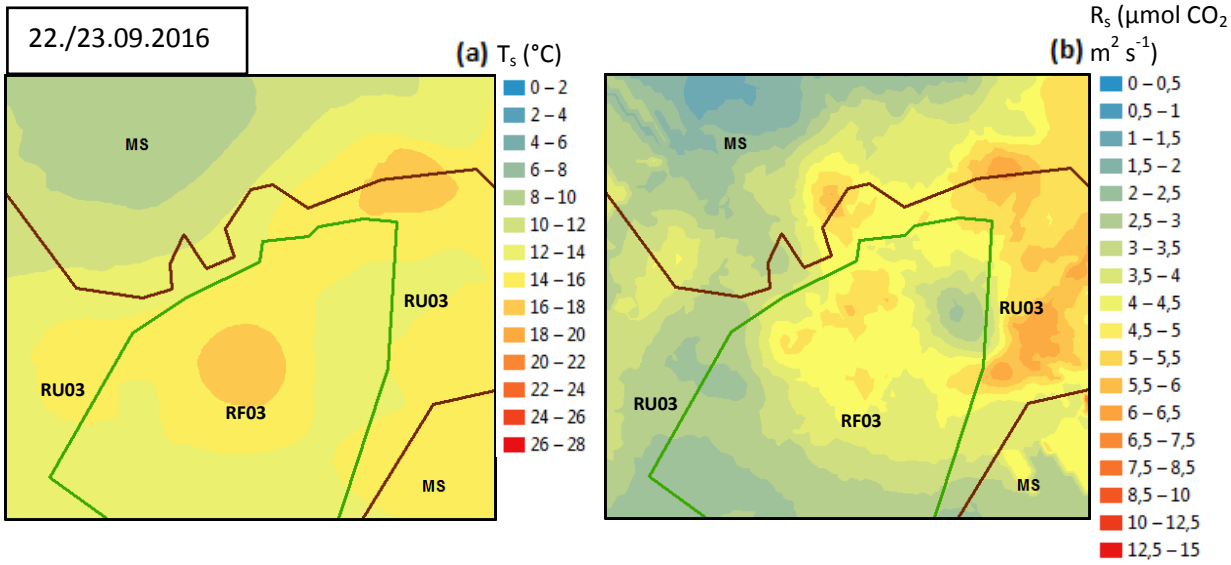

Fig. 12: Ordinal kriging map for the measured and interpolated soil temperature(T_s) (a) and soil respiration (R_s) (b) for the fifth measurement campaign at the 22./23.09.2016. The green line indicates the fenced treatment (RF03), the brown line the mature stand (MS) and the in-between area the unfenced treatment (RU03).

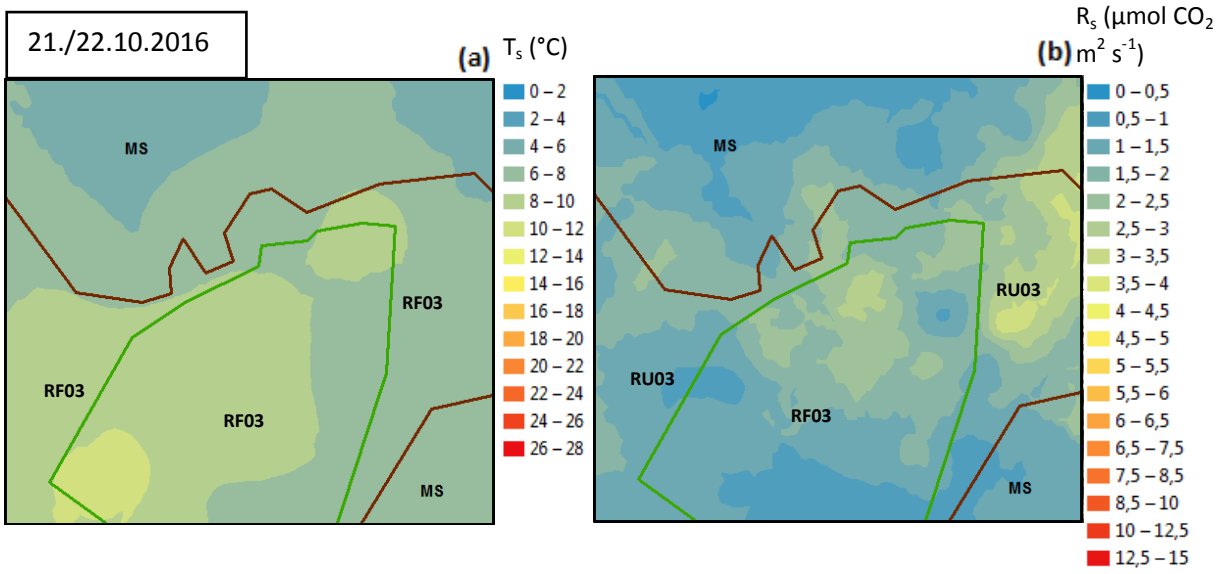

Fig. 13: Ordinal kriging map for the measured and interpolated soil temperature (T_s) (a) and soil respiration (R_s) (b) for the sixth measurement campaign at the 21./22.10.2016. The green line indicates the fenced treatment (RF03), the brown line the mature stand (MS) and the in-between area the unfenced treatment (RU03).

4. Discussion

4.1 Effects of fencing on soil CO_2 efflux, R_h, R_a and soil microclimate

Consistent with the hypothesizes, there was a clear difference between fenced and unfenced plots on the total soil respiration and its components over the observation period, especially at the later stage of succession 13 years after forest disturbance. The difference can be explained by intensive ungulate browsing at the unfenced sites, which preventing tree regeneration and altering the vegetation cover and therefore affect soil microclimatic parameters.

The measured and modeled R_s and also R_h were highly dependent on T_s at both sites and treatments (Fig. 4 a, b, d, e, Fig. 6 , Fig. 7 a, b, d, e and Table 4, 5, A1-A3 & A6-A8). Thereby, T_s explained on average 85 to 93% of the variability of R_s for the non-linear model and 79% of the variability for the ME model (Fig. 6, Table 4). This is consistent with previous studies reporting the strong positive correlation between T_s, R_s as well as R_h (Kobler et al., 2015, Mayer et al., 2017b, Zehetgruber, 2017).

However, the reason of the divergent pattern of RF03 at the third and fourth measurement campaign on the 30.07 and 22.08/23.08.2016, when the highest R_s rate was not accompanied by the highest T_s, could have been provoked by so called "hot moments". These are space restricted short-term events or sequences of events with increased biological activity of the edaphic community, e.g. triggered by the turn-over of fecal matter, optimal environmental conditions of specific microbial communities or the passing-by of earthworms (Kuzyakov and Blagodatskaya, 2015).

Hypothesis 1, in an earlier stage of succession, when dense grass layers have not been established, R_a is lower in the unfenced treatment when compared to the fenced treatment, but in later stages of succession when a dense grass layer has established outside the fence, R_a is higher in the unfenced treatment compared to the fenced treatment with tree regeneration - could be confirmed comparing the sites.

The magnitude and development over time of R_s and its components of both sites are similar to findings of other studies (Bond-Lamberty et al., 2004, Mayer et al., 2017b, Bahn et al., 2008). Mayer et al. (2017) stated an average R_s of 2.8 µmol CO_2 m^{-2} s^{-1} and an average R_a of 0.4 µmol CO_2 m^{-2} s^{-1} at the younger windthrow (HU07) 5 years after disturbance. The RaC at this time was 17%. It seems, that the successive establishment of pioneer vegetation and also

tree regeneration after 9 years of post-disturbance were responsible for the higher R_a (1.1 µmol CO_2 m^{-2} s^{-1}) as well as RaC (33%) at the Hoellengebirge site (Table A5, Fig. 5 b, c). Surprisingly, the RaC played a slightly more dominant role at HU07 (33%) compared to HF07 (28%) (Fig. 5 c), despite a scarcer aboveground vegetation. This could be traced back to the late establishment of the root exclusion plots, which were already established at HU07 in 2015. Therefore, it is likely, that roots and microorganisms associated with roots (e.g. ectomycorrhizas) at HF07 were still active and therefore biased the R_a calculation. However, focusing on the main foliation period, R_a and RaC at HF07 (40%) were higher than at HU07 (34%). In case of successful tree recovery, RaC is about 50%. Some studies suggest that R_a and RaC are closely related to gross primary production and the allocation of photosynthates to the roots (Janssens et al., 2001, Hopkins et al., 2013). According to Amiro et al. (2010), disturbed forest sites could recover within 20 years and then act as carbon sink, if tree regeneration is not inhibited. Therefore, the relatively high R_a and RaC of 40% during the foliation period at HF07 indicates a higher net ecosystem productivity than at HU07 and an adjustment to pre-disturbance conditions at the fenced treatment.

As hypothesized, the Reutte site reveals a different pattern: R_a was significantly lower at RF03 than at RU03 (Table A5, Fig. 5 e). This phenomenon of a high Ra at a late successional stage of a windthrow covered with grass but lacking tree regeneration was also observed by a former study of Mayer et al. (2014). This may have induced by the higher T_s and also the higher belowground translocation of assimilated carbon and an increased flow of root exudates of grasses compared to trees, which could also lead to higher SOC in the mineral layer (Pumpanen et al., 2004, Freschet et al., 2013, Hiltbrunner et al., 2013, Kuzyakov and Domanski, 2000). In line with this argumentation, Thuille et al. (2006) refer to significantly higher SOC stocks in mineral layers (10-20cm) of abandoned meadows compared to afforested spruce stands in Thuringia and the German Alps.

Hypothesis 2 - that R_h is higher in the unfenced treatment than in the fenced treatment because of higher microbial activity due to higher soil temperatures during the vegetation period and R_h dominating R_s - could only be confirmed at the older windthrow at the Reutte site, while at the Hoellengebirge site no significant differences in respect to R_h were detected (Table A5). Nevertheless, R_s was dominated by R_h at both sites (Fig. 5 c, f).

Despite the soil temperatures at HU07 were higher when compared to HF07 (on average + 1.5 ± 0.6 °C), R_h at HF07 was higher when compared to HU07 (Fig. 5 a & d). Additionally, VWC_s at HU07 were significantly higher during the whole measurement period and therefore

more favorable for microbial activity (Fig. 4 c). Such microclimatic patterns are a common response to disturbances (Mayer et al., 2014, Payeur-Poirier et al., 2012, Hu et al., 2017). However, at the same site Mayer et al. (2017b) reported an initial increase of R_h in the first 5 years after disturbance, mainly attributed to increased temperatures. The results of this study suggest, that the initial temperature-related increase of R_h has vanished 9 years after windthrow. The better litter quality and higher quantity of the promoted succession vegetation at HF07 may compensate for the temperature differences and enhances R_h. R_s was lower (n.s.) at HU07 compared to HF07 during the whole measurement period and tend to be significant lower ($p = 0.1006$) during the vegetation period (Table A4). This is a consequence of the relative low R_h at HU07. Mayer et al. (2014) also reported at the same study site lower R_s effluxes at HU07 5 years after disturbance when compared to an adjacent disturbance site 3 years after disturbance. This indicates, that the hampered succession vegetation and therefore low R_a effluxes in addition with the decline of more easily decomposable substrate and therefore lower R_h are responsible for the lower R_s rates at HU07 compared to HF07.

As mentioned above, the results at the Reutte site are consistent with hypothesis 2. The average R_h at RU03 is significantly higher (average $R_h = 4.71 \pm 0.26$ µmol CO_2 m^{-2} s^{-1}) than at RF03 (average $R_h = 3.43 \pm 0.20$ µmol CO_2 m^{-2} s^{-1}) (Table A5). As assumed, this could be traced back mainly to the significant T_s differences, induced by the failed tree regeneration at RU03 (Table A4). RU03 showed on average 2.2 °C higher temperatures than RF03, while between the latter and MS no significant differences could be observed. It seems that, if a successful tree establishment is still inhibited over years after disturbance and a dense grass community could establish, R_h fluxes are promoted due to microclimatic conditions but also because of the specific above- and belowground litter input of perennial grasses. The acidifying litter of coniferous species hamper the biological activity of earthworms and other deep-dwelling invertebrates, resulting in lower bioturbation and the development of thicker organic layers (Thuille and Schulze, 2006, Muys et al., 1992). Saetre (1998) reported, that the litter input in spruce forests has to be admixed with at least 25% of more easily degradable beech leaves to be an appropriate habitat for earthworms. Easy decomposable litter of herbs and grasses could have led to the change of the humus forms from Moder to Mull and to shallow O-layer depths at RU03, while at RF03 coniferous litter and lower soil temperatures promote the recovery of an ecto-organic soil layer .

However, these findings are in contrast with a study of Zehetgruber et al. (2017), who observed a decline of R_h in time since disturbance and with the establishment of a dense grass

layer. The author argued that the establishment of fast growing non-woody ground vegetation lead to lower C strength. These differences could be explained by lower temperature discrepancies between the treatments caused by the north-west exposition of the study site of Zehetgruber et al. (2017) compared to the south exposition at the sites of this study. The research sites of the cited study also differed from this study concerning the time since disturbance, which is 3 and 5 years and thus considerably shorter when compared to the sites of this study.

Due to the significantly higher R_h at RU03 compared to RF03 and MS, it is very likely that disturbed sites with failed tree regeneration act as carbon sources. This assumption is supported by several studies, which revealed significant lower SOC stocks in the organic layer at sites with inhibited tree regeneration (Mayer et al., 2014, Prietzel, 2008, Spielvogel et al., 2006). At the Reutte site R_s and R_h were significantly higher at RU03 than at RF03 during the whole measurement period as well as during the vegetation period. It is assumed that different trajectories of regeneration in fenced and unfenced plots – a canopy of tree seedlings and saplings inside and a dense grass cover outside the fence – is an effect of ungulate herbivory. The population control of ungulate herbivores thus may be an appropriate measure to reduce CO_2 emissions to the atmosphere.

The modeled Q_{10} are consistent with several other studies investigating the exponential relationship of R_s and R_h with T_s (Zu et al., 2009, Pumpanen et al., 2004, Payeur-Poirier et al., 2012). The Q_{10} of R_s and R_h ranged between 2.18 and 3.25 and 1.86 and 2.59, respectively (Table 4). Fencing increased the Q_{10} of soil respiration at disturbed sites.. This pattern as well as the magnitude of Q_{10} were also observed in studies comparing the temperature sensitivity between clear-cuts and mature stands, indicating higher temperature sensitivities at intact forest sites (Pumpanen et al., 2004, Zu et al., 2009). The Q_{10} reflects the respiration sensitivity in interdependence to T_s, but also to other factors like root biomass and substrate quality (Zu et al., 2009, Boone et al., 1998). Hence, the higher Q_{10} at the fenced strata could be traced back to 3 reasons:

First, an acclimatization of the microbial community to higher temperatures leads to lower temperature sensitivities at the unfenced treatments. This phenomenon was observed by former studies (Luo et al., 2001, Janssens and Pilegaard, 2003) and may lead to a homoeostasis (at least in a short-term perspective) of the carbon fluxes in context of global warming (Zu et al., 2009). However, a more recent study (Schindlbacher et al., 2015) investigating this "acclimatization-effect" in the Northern Calcareous Alps by a warming

experiment could not identify a microbial adaptation, primarily traced back to the high SOC content and the high quality and quantity of labile C in the soil. In contrast to the cited study, where the study site is north to north-east exposed, the research sites of the present study are south exposed. Consequently, it is very likely that the SOC content of the investigated soil at this study is lower due to ontological higher temperatures and subsequently shorter SOC-turnover rates. Anyhow, it remains unclear in which magnitude the adaptation of the microbial community has led to higher temperature sensitivities at the fenced treatments and in which extent the acclimatization of soil respiration can counteract the positive feedback of global warming.

Secondly, roots and microorganisms associated with roots can influence the temperature sensitivity. It is very likely that the total root biomass (of grasses, herbs and trees) and the biomass of ectomycorrhizal fungi of the unfenced treatments is smaller than at the fenced treatments (Mayer et al., 2017b, Stursova et al., 2014, Holden and Treseder, 2013). In an experiment investigating the driving factors of temperature sensitivity, Boone et al. (1998) pointed out that root biomass and mycorrhizal biomass positively affect the temperature sensitivity. Also Mayer et al. (2017a) found in an experiment lower Q_{10} values at gap plots compared to plots at a mature stand.

Thirdly, more complex and recalcitrant SOC pools require higher activation energies and therefore lead to higher temperature sensitivities (Davidson and Janssens, 2006). It is quite likely, that the trees already established in the fenced treatments cause a higher input of more recalcitrant (e.g. lignin, tannin) complexes than in the unfenced and grass dominated treatments (Lorenz et al., 2007, Freschet et al., 2013, Thuille and Schulze, 2006).

The plot specific model approach to calculate R_s in dependence to the measured microclimatic parameters and the synchronization of T_s and VWC_s seem to be reliable (Fig. A1-A3). Nevertheless, a statistical analysis was not considered because of the low number of measurement repetitions and the accumulated model insecurities of T_{model}, VWC_{model} and R_{model}. Because the measurements were conducted only in summer and autumn, calculations of the annual C fluxes were not possible. Despite these restrictions, the development and magnitude of R_s and the total emitted C flux during the measurement period seem to be in accordance with other studies (Mayer et al., 2014, Bahn et al., 2008). Mayer et al. (2014) reported a total carbon efflux of around 11.3 t C ha^{-1} $year^{-1}$at a site similar to RU03, which is in the range of about 720 g C m^{-2} over the measurement period of 129 days.

The range of the spatial variability of R_s - expressed as coefficient of variation (CV) - fits perfectly well with a reported study of Saiz et al. (2006). The contrasting temporal development of the spatial variation (in respect to CV) at the study sites is both interesting and hard to explain: at the Hoellengebirge site, a seasonal decline of CV was detectable over the measurement period, while the CV increased at the Reutte site, especially at MS.

The observation at the Hoellengebirge site - where at HF03 a lot of deciduous trees are admixed - may be the result of a peak of fine root production in early summer. Mainiero et al. (2010) observed a higher root biomass production of Norway spruce in late summer and in autumn, while root production at European beech reached their maximum in June/July. Similar developments were also reported in several other studies (McCormack et al., 2014, Li et al., 2013, Soe and Buchmann, 2005).

The high CV of MS even at colder temperatures could be explained by the relatively constant respiration fluxes of evergreen needleleaf forests compared to deciduous forests, even in autumn (Groenendijk et al., 2011). Therefore, it is possible that plant-associated "hot spots" at MS have driven the respiration fluxes at some plots at later measurement campaigns, thus increasing the CV. Such a seasonal increase like at MS was also reported by a study of Saiz et al. (2006), who observed a similar pattern at a 47 year old Sitka spruce stand in Central Ireland. In general, this cited study found the highest CV on days with highest temperatures, which is not in accordance with the results of the present study, neither at the Hoellengebirge site nor at the Reutte site, where no pattern was detectable.

The homoscedasticity and the normal distribution of the residuals indicate, that the modeling approach of R_{model} and its compartments as well as T_{model} and VWC_{model} are adequate to calculate the carbon fluxes at the study sites (Fig. A1-A3).While the modeled C efflux of the fenced and unfenced plot seemed to be quite similar over the whole measurement period at the younger windthrow in Höllengebirge, the unfenced treatment at the older windthrow in Reutte (RF03) emitted overall more carbon, regardless of the specific source (autotrophic or heterotrophic) (Fig. 8). While no obvious trends could be found regarding magnitude or source of emitted C at the Hoellengebirge site, the C efflux of RF03 seems to be nearly on a pre-disturbance level (around 520 gC m^{-2} during 129 days at MS, Table A9), indicating the relatively fast recovery of managed forest sites after disturbances which was also reported by Amiro et al. (2010). In contrary, the grass dominated site of RU03 emitted at the same period ~730 gC m^{-2}. Around 500 gC m^{-2} of the total C efflux originates from heterotrophic

respiration, which is far higher than the respective heterotrophic C losses at RF03 and MS (328 ± 27 and 264 ± 28 gC m^{-2}, respectively).

The analysis of the heterotrophic respiration as well as the C fluxes over the whole measurement period indicate increasing discrepancies with time after forest disturbances - if no adequate regeneration measures are taken into account - and may result in a massive C source strength at sites with failed tree regeneration. Prietzel (2008) observed at a south exposed site 15 years after disturbance a more than 75% lower OC content in the O layer at a site dominated by grasses compared to a fenced treatment, while no significant changes were found for the mineral layer. Spielvogel (2006) also reported significant declines of the OC content in the organic horizons 25 years after a bark beetle infestation and a fairly stable SOC stock in the mineral layers. Also Mayer et al. (2017a) reports the positive effect of tree regeneration on decreasing decomposition, mainly induced by lowering the soil temperatures. Nevertheless, reports on the C sink or source character of post-disturbance forest ecosystems with failed tree regeneration are very scarce. However, a meta study of Poeplau et al.(2011) investigating the effect of afforestation of abandoned meadows sites in the temperate zone revealed no clear long-term trend on mineral SOC stocks changes.

4.2 Site parameters controlling CO_2 efflux

The analysis of several biotic and abiotic parameters gave – in combination with the temperature standardized respiration fluxes at 10 °C – a more detailed insight in the behavior of soil respiration after disturbances and the influence of fencing (Table 6).

In general, RU03 showed significantly higher R_{10} values than RF03, while no differences could be detected between these treatments and MS (Fig. 9a, Table A10a). Because other influential site parameters like "soil group", "humus form" and their layer thicknesses were quite similar (Table 7), it seems that the dense grass vegetation as most dominant functional group is boosting R_{10} at RU03. This would be in line with the findings presented in the former subchapter, where the labile above- and belowground litter input of dominant functional group of grasses at RU03 has led to a faster organic matter turnover than at the RF03.

Deep mineral soils (chromic cambisols and rendzic cambic leptosols) showed higher R_{10} values than shallow organic soils (histosols and rendzic leptosols) (Fig. 9 b, Table A10 c). This could be traced back to the deeper rooting systems, the higher number of (fine) roots and

therefore higher rhizodepositions at mineral soils which may result in a higher autotrophic and heterotrophic respiration. Such carbon depositions of roots and mycorrhizal hyphae can stimulate saprotrophic microorganisms and therefore heterotrophic respiration - a mechanism also known as "priming" - which was reported in several other studies (Bader and Cheng, 2007, Janssens et al., 2010, Fontaine et al., 2007). Another reason could be, that organic soils with dark topsoils show a low albedo especially at south exposed slopes, which result in desiccation processes, therefore more unfavorable microsites and hence inhibited root activity (Pröll et al., 2015, Diaci et al., 2005). There may be also a pH effect in the bacteria to fungi ratio from mineral to more acidic organic soils. Rousk et al. (2009) reports a fivefold decrease in bacterial growth and a fivefold increase in fungal growth along a pH gradient from 8.3 to 4.0, which was accompanied by decreasing soil respiration. Furthermore, higher pH in the mineral soil also promotes the development of endogeic earthworms. Haimi and Einbork (1992) found an increase of biological activity and biomass of earthworms after a liming experiment in a coniferous forest in Finland.

Focusing on the humus forms, R_{10} was significant higher in Mull humus forms than in Moder humus forms. This finding is in accordance with the typical characterization of Mull humus as highly biological active and therefore fast litter turnover rates (Nestroy, 2011, Scheffer, 2010). Theoretically, Tangel humus should have shown the lowest R_{10} rates because of its characteristically low biological activity (Zanella, 2011), but no statistical significant differences were found between Tangel and Mull as well as Moder (Fig. 9 c, Table A10 b). Considering the high spatial heterogeneity, the distance at which the humus forms were diagnosed and the low number of Tangel humus forms (n = 3), this result should be taken with caution. Furthermore, due to the changed soil climate and the intermixture of humus layers with mineral components Tangel has temporally exhibited pronounced activity even of earthworms (personal observation).

Comparing the microtopography, accumulation locations showed significantly higher R_{10} values than depletion positions This could be explained due to the fact, that deep and mineral soils are ontologically more often developed at accumulation locations, while loss locations are generally more exhibited to erosion processes, resulting in shallow and organic soils. This is also reflected by the variable "slope" and "soil depth" in relation to R_{10}, where higher slopes show a negative correlation with R_{10} and soil depth show a positive one. The same phenomena were also observed by a study of Saiz et al. (2006) at a Sitka spruce forest.

In respect to the O-layer depth, R_{10} showed a significant negative correlation at RU03, while RF03 and MS showed significant higher slope coefficients. This could be explained by the high above-ground litter quality and the much higher root-shoot ratio of grasses when compared to trees (Hiltbrunner et al., 2013, Freschet et al., 2013). A meta study conducted by Jackson et al. (1996) pointed out, that the average root-shoot ratio of temperate grasslands is about 3.7, while the ratio of coniferous and deciduous forests is on average 0.18 and 0.23, respectively. Hence, the above-ground litter input of grasses may play a less important role regarding SOC-inputs and mineralization than the below-ground litter input. This is also confirmed by the high positive effect of thicker OA-, A and B-layer on R_{10} of the grass-dominated treatment RU03. Wei et al. (Wei et al., 2012) also reported lower SOC in the uppermost 10 cm and higher SOC contents in deeper layers of a restored grassland compared to a secondary mixed oak and pine forest at a study site at the Chinese loess plateau. At RF03 and MS, the O-layer depth correlates with significant higher R_{10} values compared to RU03. Lower temperature under tree canopy may favor the establishment of thick ecto-organic humus layers. Surprisingly RF03 shows similar slope coefficients as MS in respect to the thickness of the O-layer, which may also reflect the importance of successful tree regeneration to prevent humus losses.

The percentage of vegetation cover and grass cover showed a positive significant influence on R_{10} at all treatments, while bare soil (%) showed a significant negative influence. This result suggests higher autotrophic respiration at highly vegetated plots but also may reflect the higher litter quality and quantity of grasses compared to deciduous and needle litter at RF03 and MS (Santruckova et al., 2006).

Additionally, the variable debris cover (%) (only significant at R03) reveals interesting results: while this variable shows a negative effect on R_{10} at RU03, the inverse pattern was observed at MS while RF03 showed only a slight negative effect. One theoretical explanation could be the relation to the specific microbial communities, which may be specialized on easy degradable litter inputs of grasses at RU03. In contrast, additional debris inputs at RF03 and MS may reflect an additional nutrient source for the microorganisms, thus increasing R_{10} (Ayres et al., 2009, Milcu and Manning, 2011, Mayer et al., 2017b).

4.3 Spatial correlation and mapping of CO_2 efflux

Semivariograms of the last three measurement campaigns revealed a spatial correlation between 18.1 (October) and 28.9 meters (August), whereas the range is declining with decreasing temperature (Table 8, Fig. 10). These findings are in line with a study of (Ohashi and Gyokusen, 2007) and could be traced back to the higher variation of R_s at colder temperatures. Soe and Buchmann (2005) reported a correlation of about 6 m, which is considerably lower than in this study. However, the results indicate only moderate spatial dependencies and reflects the heterogeneous distribution of site parameters in the Northern calcareous Alps. Due to the low number of measurement repetitions at the geometrical stratified random scheme, a standardization of the microclimatic parameters and the respiration fluxes was not possible. Hence, the results of the geostatistical analysis need to be used with caution. Nevertheless, the kriging maps of the measured R_s reveal interesting patterns throughout the measurement campaign. The visualizations reflect the discussed results above and reveal that the unfenced zone as well as the fringe area of MS show considerably higher temperatures and therefore respiration fluxes when compared to the fenced zone (Fig. 11-13). Even in the flat area, characterized by deep and mineral soils – which showed a positive correlation with R_s – the efflux is drastically lower than in the adjacent unfenced area. The maps also display the high respiration rates at this accumulation zone at RU03 throughout the measurement campaign. Furthermore, the adjustment of R_s between the treatments with decreasing temperature - visible at the kriging map of October - indicates the higher root activity of the coniferous dominated treatment. The effect of ungulate herbivory on soil carbon dynamics could be visualized very well.

5. Conclusion

The results of this study show that ungulate herbivory exerts enormous effects on post disturbance soil carbon dynamics at south exposed sites in the Northern Calcareous Alps. Inhibited tree reestablishment due to intensive ungulate browsing can lead to the development of dense grass (*Calamagrostis sp*.) layers and subsequently exert a drastic influence on R_s, R_h, the temperature sensitivity and the thickness of the soil organic layer. Fluxes of R_s and R_h over the whole measurement period were about twice as high (R_s = ~ 730 gC m-² , R_h = 500 gC m-²) at the older unfenced treatment (13 years after windthrow) when compared to the younger one (9 years after windthrow) and much higher than at the respective fenced treatment (R_s = ~ 500 gC m-² , R_h = 330 gC m-²). Hence, drastic C losses due to mineralization at south exposed sites with failed tree regeneration are very likely (Prietzel, 2008, Spielvogel et al., 2006). Taking into account that the aboveground carbon assimilation of grasslands is negligible in comparison to those of trees, a huge potential carbon sink would remain unused (Thuille and Schulze, 2006). The reduction of the density of ungulate herbivores would not only reduce soil respiration rates, but also promote the recovery of an ecto-organic humus layer. This may improve the nutritional status and the water storage capacity of the site and facilitate natural regeneration (Prietzel, 2008). Additionally, promoting the recovery of disturbed forest sites could also maintain the ecosystem services associated with forests (e.g. drinking water provision, stabilization of slopes, rock fall and avalanche protection) and therefore reduce the expenditures for artificial protection measures (Reimoser, 2010, Pröll et al., 2015). Considering the presumed increase of disturbance events due to climate change, the bad condition of rejuvenation areas in Austria and need to establish C sinks to reach the goals of the Paris Climate agreement, a reduction of ungulate herbivores seems advisable. Nevertheless, further detailed research on long-term effects of ungulate herbivores on post-disturbance forest ecosystems (e.g. also including the assessment of above- and belowground C) would be desirable, to reduce controversies and uncertainties regarding the C dynamics after forest disturbance events in the Northern Calcareous Alps.

6. Abstract

Ungulate herbivores play a crucial role in the establishment of tree regeneration after forest disturbance and can affect soil carbon dynamics. Despite the presumed increase of disturbance events with changing climate and the lack of regeneration at big parts of Austrian forests – induced by the high density of ungulate herbivores – information about the effect of ungulate herbivores on soil respiration and its components is sparse. Measurements of soil respiration (R_s) and its autotrophic (R_a) and heterotrophic (R_h) components were conducted at two south-exposed, windthrown forest sites in the Northern Calcareous Alps 9 and 13 years after disturbance during the vegetation period of 2016. Each site was divided into an unfenced (UF) and a fenced (FE) treatment to account for the influence of ungulate herbivores. At the older site, an adjacent mature spruce forest was used as control stand. To distinguish R_a and R_h, root-exclusion plots were established. Biotic and abiotic site parameters were assessed in order to analyze their effect on R_s. Spatial dependencies of R_s were analyzed and illustrated by means of semivariograms and ordinal kriging. Results indicate a successive increase in R_s and its autotrophic and heterotrophic components, if tree regeneration is inhibited due to ungulate browsing and grasses predominate. R_a did not differ significantly ($p < 0.05$), neither in the younger nor the older stand during the whole measurement period, while R_s and R_h at the older UF was significantly higher when compated to the respective FE. Lower temperature sensitivities indicate that the higher R_h are likely explained by the high quality and quantity of the dense grassy vegetation at the UF and the higher soil temperatures (T_s). At both sites, higher T_s (only significant at the older site) could be detected at UF when compared to FE, induced by the missing canopy closure. Estimated R_h of ~500 gC m^{-2} at UF and Rh of ~330 gC m^{-2} at the corresponding FE at the older disturbance site during the observation period of 129 days indicate massive soil carbon losses induced by ungulate browsing. Linear models confirm that soil basal respiration at 10 °C depends on micro-topography, soil and humus characteristics and is positively influenced by grass cover. The analysis of spatial dependence revealed only moderate dependencies, induced by the heterogeneity of the sites. The results implicate that due to the missing long-term aboveground carbon assimilation of grass vegetation and the high R_h, high densities of ungulate herbivores on post-disturbance forest sites increase atmospheric CO_2 concentrations. This illustrates the need for proactive forest management in times of climate warming.

7. Zusammenfassung

Überhöhte Wildbestände können nach Störungsereignissen die Verjüngung von Waldökosystemen hemmen und infolgedessen massiven Einfluss auf Bodenkohlenstoffdynamiken ausüben. Für ein Verständnis der Mechanismen sind derzeit zu wenige empirische Arbeiten über die durch Herbivorie veränderte sekundäre Sukzession und dadurch geänderte Bodenkohlenstoffdynamik vorhanden, was in Anbetracht der angenommen erhöhten Frequenz und Intensität von Störungsregimen durch den Klimawandel und dem aktuellen Verjüngungsdefizit großer Teile des österreichischen Waldes an Bedeutung gewinnt. Daher wurden in dieser Studie die Bodenrespiration (R_s) und deren autotrophe (R_a) sowie heterotrophe (R_h) Bestandteile 9 bzw. 13 Jahre nach Windwürfen an zwei südexponierten Waldflächen in den nördlichen Kalkalpen während der Vegetationsperiode 2016 untersucht. Um den Wildeinfluss zu quantifizieren wurde an beiden Standorten innerhalb (FE) als auch außerhalb (UF) einer umzäunten Fläche Messpunkte etabliert. Zudem wurde an dem älteren Standort eine weitere Fläche in einem Fichtenaltbestand als Kontrollzone ausgewiesen. Die Differenzierung der R_a und R_h erfolgte mittels Trenching-Methode. Zudem wurde eine detaillierte Standortsbeschreibung der älteren Versuchsfläche durchgeführt, um den Einfluss biotischer wie abiotischer Standortsparameter auf die Bodenrespiration zu untersuchen. Eine Analyse und Visualisierung der räumlichen Abhängigkeit der Respiration wurde mittels Semivariogrammen und ordinal Kriging durchgeführt. Die Ergebnisse weisen einen sukzessiven Anstieg von R_s und deren Bestandteile auf, wenn Verjüngung durch Wildverbiss unterbunden wird und die Flächen vergrasen. R_a unterschied sich auf beiden Versuchsflächen nicht signifikant zwischen UF und FE über die gesamte Messperiode, während auf der älteren Fläche R_s und R_h in UF signifikant höher waren. Höhere R_h lassen sich auf höhere Bodentemperaturen aufgrund des fehlenden Kronenschlusses in UF (signifikant auf der älteren Versuchsfläche) und die bessere Qualität und Quantität des eingetragenen Materials zurückführen, was auf massive Bodenkohlenstoffverluste hinweist. Eine Schätzung ergab eine R_h von ~500 gC m^{-2} über die gesamte Messperiode in der älteren UF und ~330 gC m^{-2} in der nebenanliegenden FE, was nahezu dem Niveau des Altbestandes entspricht (~260 gC m^{-2}). In statistischen Modellen erklären Standortparameter wie Bodentyp, Humusform und Mikrotopographie einen Teil der Variabilität der Bodenatmung bei 10 °C, zusätzlich zeigte die Grasbedeckung einen signifikanten positiven Einfluss. Die geostatische Analyse ergab moderate räumliche Abhängigkeiten, was auf die Heterogenität der Versuchsflächen zurückzuführen ist. Die

fehlende Kohlenstoffassimilierung in der oberirdischen Biomasse und die gesteigerte R_h auf ungezäunten Flächen zeigen, dass hohe Wilddichten auf Störungsflächen einen Anstieg der atmosphärische CO_2-Konzentration nach sich ziehen können. Dies verdeutlicht die Wichtigkeit eines aktiven Waldmanagements in Zeiten der Klimaerwärmung.

8. References

AMIRO, B. D., BARR, A. G., BARR, J. G., BLACK, T. A., BRACHO, R., BROWN, M., CHEN, J., CLARK, K. L., DAVIS, K. J., DESAI, A. R., DORE, S., ENGEL, V., FUENTES, J. D., GOLDSTEIN, A. H., GOULDEN, M. L., KOLB, T. E., LAVIGNE, M. B., LAW, B. E., MARGOLIS, H. A., MARTIN, T., MCCAUGHEY, J. H., MISSON, L., MONTES-HELU, M., NOORMETS, A., RANDERSON, J. T., STARR, G. & XIAO, J. 2010. Ecosystem carbon dioxide fluxes after disturbance in forests of North America. *Journal of Geophysical Research-Biogeosciences,* 115, G002K02.

AYRES, E., STELTZER, H., SIMMONS, B. L., SIMPSON, R. T., STEINWEG, J. M., WALLENSTEIN, M. D., MELLOR, N., PARTON, W. J., MOORE, J. C. & WALL, D. H. 2009. Home-field advantage accelerates leaf litter decomposition in forests. *Soil Biology & Biochemistry,* 41**,** 606-610.

BADER, N. E. & CHENG, W. X. 2007. Rhizosphere priming effect of Populus fremontii obscures the temperature sensitivity of soil organic carbon respiration. *Soil Biology & Biochemistry,* 39**,** 600-606.

BAHN, M., RODEGHIERO, M., ANDERSON-DUNN, M., DORE, S., GIMENO, C., DROSLER, M., WILLIAMS, M., AMMANN, C., BERNINGER, F., FLECHARD, C., JONES, S., BALZAROLO, M., KUMAR, S., NEWESELY, C., PRIWITZER, T., RASCHI, A., SIEGWOLF, R., SUSILUOTO, S., TENHUNEN, J., WOHLFAHRT, G. & CERNUSCA, A. 2008. Soil Respiration in European Grasslands in Relation to Climate and Assimilate Supply. *Ecosystems,* 11**,** 1352-1367.

BMLFUW 2013. THE AUSTRIAN STRATEGY FOR ADAPTION TO CLIMATE CHANGE. Stubenbastei 5, 1010 Vienna.

BOND-LAMBERTY, B. & THOMSON, A. 2010. Temperature-associated increases in the global soil respiration record. Nature, 464, 579-582.

BOND-LAMBERTY, B., WANG, C. K. & GOWER, S. T. 2004. Contribution of root respiration to soil surface CO(2) flux in a boreal black spruce chronosequence. *Tree Physiology,* 24**,** 1387-1395.

BOONE, R. D., NADELHOFFER, K. J., CANARY, J. D. & KAYE, J. P. 1998. Roots exert a strong influence on the temperature sensitivity of soil respiration. *Nature,* 396**,** 570-572.

CAMBARDELLA, C. A., MOORMAN, T. B., NOVAK, J. M., PARKIN, T. B., KARLEN, D. L., TURCO, R. F. & KONOPKA, A. E. 1994. FIELD-SCALE VARIABILITY OF SOIL PROPERTIES IN CENTRAL IOWA SOILS. *Soil Science Society of America Journal,* 58**,** 1501-1511.

CERNY, K. 2000. Biotopkartierung der Gemeinde Höfen. Amt der Tiroler Landesregierung, Abteilung Umweltschutz.

CRESSIE, N. & HAWKINS, D. M. 1980. ROBUST ESTIMATION OF THE VARIOGRAM .1. *Journal of the International Association for Mathematical Geology,* 12**,** 115-125.

DAVIDSON, E. A. & JANSSENS, I. A. 2006. Temperature sensitivity of soil carbon decomposition and feedbacks to climate change. *Nature,* 440**,** 165-173.

DIACI, J., PISEK, R. & BONCINA, A. 2005. Regeneration in experimental gaps of subalpine Picea abies forest in the Slovenian Alps. *European Journal of Forest Research,* 124**,** 29-36.

ELLENBERG, H. 1992. Zeigerwerte der Pflanzen in Mitteleuropa. Göttingen: Scripta Geobotanica 18.

FAO 2015. World reference base for soil resources 2014. *International soil classification system for naming soils and creating legends for soil maps.* Rome: Food and Agriculture organization of the United Nations.

FONTAINE, S., BAROT, S., BARRE, P., BDIOUI, N., MARY, B. & RUMPEL, C. 2007. Stability of organic carbon in deep soil layers controlled by fresh carbon supply. *Nature,* 450**,** 277-U10.

FRESCHET, G. T., CORNWELL, W. K., WARDLE, D. A., ELUMEEVA, T. G., LIU, W. D., JACKSON, B. G., ONIPCHENKO, V. G., SOUDZILOVSKAIA, N. A., TAO, J. P. & CORNELISSEN, J. H. C. 2013. Linking litter decomposition of above- and below-ground organs to plant-soil feedbacks worldwide. *Journal of Ecology,* 101**,** 943-952.

FULLER, R. J. & GILL, R. M. A. 2001. Ecological impacts of increasing numbers of deer in British woodland. *Forestry,* 74**,** 193-199.

GROENENDIJK, M., DOLMAN, A. J., AMMANN, C., ARNETH, A., CESCATTI, A., DRAGONI, D., GASH, J. H. C., GIANELLE, D., GIOLI, B., KIELY, G., KNOHL, A., LAW, B. E., LUND, M., MARCOLLA, B., VAN DER MOLEN, M. K., MONTAGNANI, L., MOORS, E., RICHARDSON, A. D., ROUPSARD, O., VERBEECK, H. & WOHLFAHRT, G. 2011. Seasonal variation of photosynthetic model parameters and leaf area index from global Fluxnet eddy covariance data. *Journal of Geophysical Research-Biogeosciences,* 116, G04027.

HANSON, P. J., EDWARDS, N. T., GARTEN, C. T. & ANDREWS, J. A. 2000. Separating root and soil microbial contributions to soil respiration: A review of methods and observations. *Biogeochemistry,* 48**,** 115-146.

HAIMI, J., EINBORK, M. 1992. Effects of endogeic earthworms on soil processes and plant growth in coniferous forest soils. *Biology and Fertility of Soils*, 13, 6-10.

HILTBRUNNER, D., ZIMMERMANN, S. & HAGEDORN, F. 2013. Afforestation with Norway spruce on a subalpine pasture alters carbon dynamics but only moderately affects soil carbon storage. *Biogeochemistry,* 115**,** 251-266.

HOLDEN, S. R. & TRESEDER, K. K. 2013. A meta-analysis of soil microbial biomass responses to forest disturbances. *Frontiers in Microbiology,* 4(163), 1-18

HOPKINS, F., GONZALEZ-MELER, M. A., FLOWER, C. E., LYNCH, D. J., CZIMCZIK, C., TANG, J. W. & SUBKE, J. A. 2013. Ecosystem-level controls on root-rhizosphere respiration. *New Phytologist,* 199**,** 339-351.

HOTTER, M. 2013. Waldtypisierung in Tirol. *In:* SIMON, A., VACIK, H. (ed.) *Definitionen und Begriffe.* Innsbruck: Amt der Tiroler Landesregierung, Abteilung Forst.

HU, T. X., SUN, L., HU, H. Q., WEISE, D. R. & GUO, F. T. 2017. Soil Respiration of the Dahurian Larch (Larix gmelinii) Forest and the Response to Fire Disturbance in the Daxing'an Mountains, China. *Plos One*, 12, e0180214.

JACKSON, R. B., CANADELL, J., EHLERINGER, J. R., MOONEY, H. A., SALA, O. E. & SCHULZE, E. D. 1996. A global analysis of root distributions for terrestrial biomes. *Oecologia,* 108**,** 389-411.

JANSSENS, I. A., DIELEMAN, W., LUYSSAERT, S., SUBKE, J. A., REICHSTEIN, M., CEULEMANS, R., CIAIS, P., DOLMAN, A. J., GRACE, J., MATTEUCCI, G., PAPALE, D., PIAO, S. L., SCHULZE, E. D., TANG, J. & LAW, B. E. 2010. Reduction of forest soil respiration in response to nitrogen deposition. *Nature Geoscience,* 3**,** 315-322.

JANSSENS, I. A., LANKREIJER, H., MATTEUCCI, G., KOWALSKI, A. S., BUCHMANN, N., EPRON, D., PILEGAARD, K., KUTSCH, W., LONGDOZ, B., GRUNWALD, T., MONTAGNANI, L., DORE, S., REBMANN, C., MOORS, E. J., GRELLE, A., RANNIK, U., MORGENSTERN, K., OLTCHEV, S., CLEMENT, R., GUDMUNDSSON, J., MINERBI, S., BERBIGIER, P., IBROM, A., MONCRIEFF, J., AUBINET, M., BERNHOFER, C., JENSEN, N. O., VESALA, T., GRANIER, A., SCHULZE, E. D., LINDROTH, A., DOLMAN, A. J., JARVIS, P. G., CEULEMANS, R. & VALENTINI, R. 2001. Productivity overshadows temperature in determining

soil and ecosystem respiration across European forests. *Global Change Biology,* 7**,** 269-278.

JANSSENS, I. A. & PILEGAARD, K. 2003. Large seasonal changes in Q(10) of soil respiration in a beech forest. *Global Change Biology,* 9**,** 911-918.

KILIAN, F. 1994. Die forstlichen Wuchsgebiete Österreichs - Eine Naturraumgliederung nach waldökologischen Gesichtspunkten. *In:* MÜLLER F, S. F. (ed.). Vienna: Austrian Research Center for Forests.

KIRSCHBAUM, M. U. F., EAMUS, D., GIFFORD, R.M., ROXBURG, S.H., SANDS, P.J. 2001. Definitions of some ecological terms commonly used in carbon accounting. In: Kirschbaum, M.U.F., Mueller, R. (Eds.), Net Ecosystem Exchange. Cooperative Research Centre for Greenhouse Accounting. Canberra, Australia.

KNOHL, A., SOE, A. R. B., KUTSCH, W. L., GOCKEDE, M. & BUCHMANN, N. 2008. Representative estimates of soil and ecosystem respiration in an old beech forest. *Plant and Soil,* 302**,** 189-202.

KOBLER, J., JANDL, R., DIRNBOCK, T., MIRTL, M. & SCHINDLBACHER, A. 2015. Effects of stand patchiness due to windthrow and bark beetle abatement measures on soil CO2 efflux and net ecosystem productivity of a managed temperate mountain forest. *European Journal of Forest Research,* 134**,** 683-692.

KUULUVAINEN, T., KALMARI, R. 2003. Regeneration microsites of Picea abies seedlings in a windthrow area of a boreal old-growth forest in southern Finland. *Annales Botanici Fennici,* 40**,** 401-413.

KUZYAKOV, Y. & BLAGODATSKAYA, E. 2015. Microbial hotspots and hot moments in soil: Concept & review. *Soil Biology & Biochemistry,* 83**,** 184-199.

KUZYAKOV, Y. & DOMANSKI, G. 2000. Carbon input by plants into the soil. Review. *Journal of Plant Nutrition and Soil Science-Zeitschrift Fur Pflanzenernahrung Und Bodenkunde,* 163**,** 421-431.

LAND TIROL, 2017. Tiris - Tiroler Rauminformationssystem.

LI, X. F., ZHU, J., LANGE, H. & HAN, S. J. 2013. A modified ingrowth core method for measuring fine root production, mortality and decomposition in forests. *Tree Physiology,* 33**,** 18-25.

LINDROTH, A., LAGERGREN, F., GRELLE, A., KLEMEDTSSON, L., LANGVALL, O., WESLIEN, P. & TUULIK, J. 2009. Storms can cause Europe-wide reduction in forest carbon sink. *Global Change Biology,* 15**,** 346-355.

LLOYD, J. & TAYLOR, J. A. 1994. ON THE TEMPERATURE-DEPENDENCE OF SOIL RESPIRATION. *Functional Ecology,* 8**,** 315-323.

LORENZ, K., LAL, R., PRESTON, C. M. & NIEROP, K. G. J. 2007. Strengthening the soil organic carbon pool by increasing contributions from recalcitrant aliphatic bio(macro)molecules. *Geoderma,* 142**,** 1-10.

LUO, Y. Q., WAN, S. Q., HUI, D. F. & WALLACE, L. L. 2001. Acclimatization of soil respiration to warming in a tall grass prairie. *Nature,* 413**,** 622-625.

MAINIERO, R., KAZDA, M. & SCHMID, I. 2010. Fine root dynamics in 60-year-old stands of Fagus sylvatica and Picea abies growing on haplic luvisol soil. *European Journal of Forest Research,* 129**,** 1001-1009.

MATHERON, G. 1963. Principles of geostatistics. Economic Geology 58: 1246-1266.

MAYER, M., MATTHEWS, B., ROSINGER, C., SANDEN, H., GODBOLD, D. L. & KATZENSTEINER, K. 2017a. Tree regeneration retards decomposition in a temperate mountain soil after forest gap disturbance. *Soil Biology & Biochemistry,* 115**,** 490-498.

MAYER, M., MATTHEWS, B., SCHINDLBACHER, A. & KATZENSTEINER, K. 2014. Soil CO2 efflux from mountainous windthrow areas: dynamics over 12 years post-disturbance. *Biogeosciences,* 11**,** 6081-6093.

MAYER, M., SANDEN, H., REWALD, B., GODBOLD, D. L. & KATZENSTEINER, K. 2017b. Increase in heterotrophic soil respiration by temperature drives decline in soil organic carbon stocks after forest windthrow in a mountainous ecosystem (vol 31, pg 1163, 2017). *Functional Ecology,* 31**,** 1669-1669.

MCCORMACK, M. L., ADAMS, T. S., SMITHWICK, E. A. H. & EISSENSTAT, D. M. 2014. Variability in root production, phenology, and turnover rate among 12 temperate tree species. *Ecology,* 95**,** 2224-2235.

MILCU, A. & MANNING, P. 2011. All size classes of soil fauna and litter quality control the acceleration of litter decay in its home environment. *Oikos,* 120**,** 1366-1370.

MUYS, B., LUST, N. & GRANVAL, P. 1992. Effects of grassland afforestation with different tree species on earthworm communities, litter decomposition and nutrient status. *Soil Biology & Biochemistry,* 24**,** 1459-1466.

NESTROY, O. 2011. Systematische Gliederung der Böden Österreichs. *In:* DANNEBERG, O. H., ENGLISCH, M., GEßL, A., HAGER, H., HERZBERGER, E., KILIAN, W., & NELHIEBEL, P., PECINA, E., PEHAMBERGER, A., SCHNEIDER, W., AND WAGNER, J. (eds.) *Österreichische Bodensystematik in der revidierten Fassung von 2011.* Vienna.

OHASHI, M. & GYOKUSEN, K. 2007. Temporal change in spatial variability of soil respiration on a slope of Japanese cedar (Cryptomeria japonica D. Don) forest. *Soil Biology & Biochemistry,* 39**,** 1130-1138.

PAYEUR-POIRIER, J. L., COURSOLLE, C., MARGOLIS, H. A. & GIASSON, M. A. 2012. CO2 fluxes of a boreal black spruce chronosequence in eastern North America. *Agricultural and Forest Meteorology,* 153**,** 94-105.

PINHEIRO, J. C., BATES, D.M. 2000. Mixed Effects models in S and S-Plus. Berlin: Springer - Verlag.

POEPLAU, C., DON, A., VESTERDAL, L., LEIFELD, J., VAN WESEMAEL, B., SCHUMACHER, J. & GENSIOR, A. 2011. Temporal dynamics of soil organic carbon after land-use change in the temperate zone - carbon response functions as a model approach. *Global Change Biology,* 17**,** 2415-2427.

PREM, J. 2016. Österreichischer Waldbericht 2015. *In:* THOMAS BASCHNY, R. B., FRANZ ESSL, ALEXANDER FOGLAR-DEINHARDSTEIN,, THOMAS GEBUREK, G. G., ALFRED GRIESHOFER, INGWALD GSCHWANDTL, J. H., RONALD HUBER, JOHANN, KIESSLING, A. K., FERDINAND LEITNER, STEFANIE LINSER, RUDOLF, LOTTERSTÄDTER, K. N., PETER MAYER, ANDREA MOSER, ANDREAS PICHLER, V.-C., PIRIBAUER, H., PÜLZL, G. R., SUSANNE ROTH, MATTHIAS SCHERMAIER, BERNHARD, SCHWARZL, W. S., ANTON TRZESNIOWSKI, PETER WEISS, MARTIN & WÖHRLE, B. W. (eds.). Vienna: Republik Österreich, Bundesministerium für Land- und Forstwirtschaft, Umwelt und Wasserwirtschaft,.

PRIETZEL, J., AMMER, C. 2008. Montane Bergmischwälder der Bayerischen Kalkalpen: Reduktion der Schalenwilddichte steigert nicht nur den Verjüngungserfolg, sondern auch die Bodenfruchtbarkeit. Allg Forst Jagdztg 179:104–112.

PRIETZEL, J. & CHRISTOPHEL, D. 2014. Organic carbon stocks in forest soils of the German Alps. *Geoderma,* 221**,** 28-39.

PRÖLL, G., DARABANT, A., GRATZER, G. & KATZENSTEINER, K. 2015. Unfavourable microsites, competing vegetation and browsing restrict post-disturbance

tree regeneration on extreme sites in the Northern Calcareous Alps. *European Journal of Forest Research,* 134**,** 293-308.

PUMPANEN, J., WESTMAN, C. J. & ILVESNIEMI, H. 2004. Soil CO2 efflux from a podzolic forest soil before and after forest clear-cutting and site preparation. *Boreal Environment Research,* 9**,** 199-212.

RAICH, J. W. & SCHLESINGER, W. H. 1992. THE GLOBAL CARBON-DIOXIDE FLUX IN SOIL RESPIRATION AND ITS RELATIONSHIP TO VEGETATION AND CLIMATE. *Tellus Series B-Chemical and Physical Meteorology,* 44**,** 81-99.

REICHSTEIN, M. & BEER, C. 2008. Soil respiration across scales: The importance of a model-data integration framework for data interpretation. *Journal of Plant Nutrition and Soil Science,* 171**,** 344-354.

REIMOSER, F., REIMOSER, S. 2010. Ungulates and their management in Austria. in: European Ungulates and their Manageent in the 21th century, edited by: Apollonop, M., Andersen, A., and Putman, P.,Cambridge University Press, 338-356.

ROUSK, J., BROOKES, P.C., BAATH E. 2009. Contrasting soil pH effects on fungal and bacterial growth suggest functional redundancy in carbon mineralization. *Applied and Environmental Microbiology*, 75, 1589-1596.

SAETRE, P. 1998. Decomposition, microbial community structure, and earthworm effects along a birch-spruce soil gradient. *Ecology,* 79**,** 834-846.

SAIZ, G., GREEN, C., BUTTERBACH-BAHL, K., KIESE, R., AVITABILE, V. & FARRELL, E. P. 2006. Seasonal and spatial variability of soil respiration in four Sitka spruce stands. *Plant and Soil,* 287**,** 161-176.

SANTRUCKOVA, H., KRISTUFKOVA, M. & VANEK, D. 2006. Decomposition rate and nutrient release from plant litter of Norway spruce forest in the Bohemian Forest. *Biologia,* 61**,** 499-508.

SCHARLEMANN, J. P. W., TANNER, E. V. J., HIEDERER, R. & KAPOS, V. 2014. Global soil carbon: understanding and managing the largest terrestrial carbon pool. *Carbon Management,* 5**,** 81-91.

SCHEFFER, F., SCHACHTSCHABEL, P. 2010. Lehrbuch der Bodenkunde. *In:* BLUME, H.-P., BÜMMER, G.W., HORN, R., KANDELER, E., KÖGEL-KNABNER, I., KRETZSCHMAR, R., STAHR, K., WILKE, B.-M. (ed.). Heidelberg: Spektrum Akademischer Verlag.

SCHELHAAS, M. J., HENGEVELD, G., MORIONDO, M., REINDS, G. J., KUNDZEWICZ, Z. W., TER MAAT, H. & BINDI, M. 2010. Assessing risk and adaptation options to fires and windstorms in European forestry. *Mitigation and Adaptation Strategies for Global Change,* 15**,** 681-701.

SCHINDLBACHER, A., SCHNECKER, J., TAKRITI, M., BORKEN, W. & WANEK, W. 2015. Microbial physiology and soil CO2 efflux after 9 years of soil warming in a temperate forest - no indications for thermal adaptations. *Global Change Biology,* 21**,** 4265-4277.

SCHINDLBACHER, A., ZECHMEISTER-BOLTENSTERN, S., KITZLER, B. & JANDL, R. 2008. Experimental forest soil warming: response of autotrophic and heterotrophic soil respiration to a short-term 10 degrees C temperature rise. *Plant and Soil,* 303**,** 323-330.

SEIDL, R., SCHELHAAS, M. J., RAMMER, W. & VERKERK, P. J. 2014. Increasing forest disturbances in Europe and their impact on carbon storage. *Nature Climate Change,* 4**,** 930-930.

SEIDL, R., THOM, D., KAUTZ, M., MARTIN-BENITO, & D., P., M., VACCHIANO, G., WILD, J., ASCOLI, D., PETR, M., HONKANIEMI J. 2017. Forest disturbance under climate change. *Nature Climate Change,* 7, 395-402.

SOE, A. R. B. & BUCHMANN, N. 2005. Spatial and temporal variations in soil respiration in relation to stand structure and soil parameters in an unmanaged beech forest. *Tree Physiology,* 25**,** 1427-1436.

SPIELVOGEL, S., PRIETZEL, J. & KOGEL-KNABNER, I. 2006. Soil organic matter changes in a spruce ecosystem 25 years after disturbance. *Soil Science Society of America Journal,* 70**,** 2130-2145.

STOYAN, H., DE-POLLI, H., BOHM, S., ROBERTSON, G. P. & PAUL, E. A. 2000. Spatial heterogeneity of soil respiration and related properties at the plant scale. *Plant and Soil,* 222**,** 203-214.

STURSOVA, M., SNAJDR, J., CAJTHAML, T., BARTA, J., SANTRUCKOVA, H. & BALDRIAN, P. 2014. When the forest dies: the response of forest soil fungi to a bark beetle-induced tree dieback. *Isme Journal,* 8**,** 1920-1931.

SUBKE, J.-A., INGLIMA, I. & COTRUFO, M. F. 2006. Trends and methodological impacts in soil CO2 efflux partitioning: A metaanalytical review. *Global Change Biology,* 12**,** 921-943.

THUILLE, A. & SCHULZE, E. D. 2006. Carbon dynamics in successional and afforested spruce stands in Thuringia and the Alps. *Global Change Biology,* 12**,** 325-342.

TIAN, H. Q., LU, C. Q., YANG, J., BANGER, K., HUNTZINGER, D. N., SCHWALM, C. R., MICHALAK, A. M., COOK, R., CIAIS, P., HAYES, D., HUANG, M. Y., ITO, A., JAIN, A. K., LEI, H. M., MAO, J. F., PAN, S. F., POST, W. M., PENG, S. S., POULTER, B., REN, W., RICCIUTO, D., SCHAEFER, K., SHI, X. Y., TAO, B., WANG, W. L., WEI, Y. X., YANG, Q. C., ZHANG, B. W. & ZENG, N. 2015. Global patterns and controls of soil organic carbon dynamics as simulated by multiple terrestrial biosphere models: Current status and future directions. *Global Biogeochemical Cycles,* 29**,** 775-792.

VACIK, H. & LEXER, M. J. 2001. Application of a spatial decision support system in managing the protection forests of Vienna for sustained yield of water resources. *Forest Ecology and Management,* 143**,** 65-76.

WEBSTER, R., OLIVER, M. 2001. Geostatistics for Environmental Scientists. West Sussex, England: John Wiley & Sons, Ltd.

WEI, J., CHENG, J. M., LI, W. J. & LIU, W. G. 2012. Comparing the Effect of Naturally Restored Forest and Grassland on Carbon Sequestration and Its Vertical Distribution in the Chinese Loess Plateau. *Plos One,* 7, e40123.

WICKHAM, H. 2009. ggplot2: Elegant Graphics for Data Analysis. New York: Springer-Verlag.

WILDBURGER, C. 2005. Auswirkungen der Jagd auf den Wald in Österreich. Eine Studie zum Einfluss der Schalenwildbewirtschaftung auf Waldökosysteme. *In:* LEBENITZ, R. (ed.). Umweltbundesamt Wien.

WRB, I. W. G. 2015. World Reference Base for Soil Resources 2014, update 2015. World Soil Resources Reports No. 106. FAO, Rome.

YUSTE, J. C., NAGY, M., JANSSENS, I. A., CARRARA, A. & CEULEMANS, R. 2005. Soil respiration in a mixed temperate forest and its contribution to total ecosystem respiration. *Tree Physiology,* 25**,** 609-619.

ZAMG 2017. Climate data for the weather stations ´Reutte´, ´Feuerkogel´ and ´Bad Ischl´. Vienna.

ZANELLA, A., JABIOL, B., PONGE, J.F., SARTORI, G., DE WAAL, R., VAN DELFT, B., GRAEFE, U., N., COOLS, N., KATZENSTEINER, K., HAGER, H., ENGLISCH, M., BRETHES, A., BROLL, G., GOBAT,, J.M., B., J.J., MILBERT, G., KOLB, E., WOLF , U., FRIZZERA , L., GALVAN, P., KOLLI , R., BARITZ, R., KEMMERS , R., VACCA, A., SERRA , G., BANAS, D., GARLATO, A., CHERSICH, S., & KLIMO, E., AND LANGOHR, R. 2011. European Humus Reference Base. HAL hal-005414(version2): 1-56.

ZEHETGRUBER, B., KOBLER, J., DIRNBLCK, T., JANDL, R., SEIDL, R., SCHINDLBACHER, A. 2017. Intensive ground vegetation growth mitigates the carbon loss after forest disturbance. Plant and Soil, 420, 239-252.

ZU, Y. G., WANG, W. J., WANG, H. M., LIU, W., CUI, S. & KOIKE, T. 2009. Soil CO2 efflux, carbon dynamics, and change in thermal conditions from contrasting clear-cut sites during natural restoration and uncut larch forests in northeastern China. *Climatic Change,* 96**,** 137-159.

9. Appendix

Table A1: Summary statistics of campaign wise measured soil respiration (R_s), soil temperature (T_s) and volumetric water content (VWC_s) for the whole site, the unfenced treatment (UF) and the fenced treatment (FE) at the Hoellengebirge.

Hoellengebirge		R_s (µmol CO_2 m^{-2} s^{-1})						T_s (°C)						VWC_s (%)					
	RecNo	mean	SD	CV	SE	Min	Max	mean	SD	CV	SE	Min	Max	mean	SD	CV	SE	Min	Max
	1	1.86	0.79	42.36	0.13	0.69	3.66	10.82	2.93	27.12	0.47	5.10	16.40	37.63	5.62	14.94	0.90	25.81	48.40
	2	1.01	0.60	58.63	0.10	0.25	2.52	14.17	3.53	24.89	0.56	8.60	22.40	34.16	3.41	9.99	0.55	26.70	41.98
	3	4.00	1.71	42.65	0.27	0.57	8.02	15.62	1.80	11.50	0.29	13.10	19.90	40.16	3.08	7.66	0.49	34.23	46.10
	4	6.32	2.46	38.94	0.40	1.01	10.16	20.15	2.53	12.57	0.41	16.90	27.50	34.86	2.90	8.33	0.47	29.23	41.60
	5	4.81	2.35	48.82	0.38	1.58	12.37	20.05	2.51	12.53	0.40	16.10	26.30	31.45	3.52	11.18	0.56	24.98	40.70
	6	3.66	1.79	48.75	0.29	0.44	10.60	14.76	2.06	13.99	0.33	11.80	20.90	32.28	5.90	18.28	0.94	24.48	54.40
	7	2.27	0.91	40.03	0.15	1.07	4.92	11.07	1.85	16.74	0.30	7.90	14.80	33.69	3.89	11.53	0.62	27.31	41.50
		R_s (µmol CO_2 m^{-2} s^{-1})						T_s (°C)						VWC_s (%)					
Hoellengebirge	RecNo	mean	SD	CV	SE	Min	Max	mean	SD	CV	SE	Min	Max	mean	SD	CV	SE	Min	Max
UF	1	2.19	0.74	34.03	0.16	0.76	3.66	9.55	2.93	30.74	0.61	5.10	16.20	41.11	3.66	8.89	0.76	33.10	48.40
	2	1.08	0.70	64.65	0.15	0.32	2.52	14.43	4.06	28.15	0.85	9.20	22.40	34.80	3.37	9.68	0.70	26.70	40.10
	3	3.84	1.87	48.60	0.39	0.57	8.02	16.53	1.79	10.81	0.37	13.10	19.90	40.10	3.00	7.49	0.63	34.23	46.10
	4	5.80	2.47	42.60	0.53	1.01	9.85	21.06	2.92	13.85	0.62	17.50	27.50	35.21	2.67	7.58	0.57	31.23	41.20
	5	4.38	1.97	45.06	0.41	1.58	8.33	20.91	2.81	13.46	0.59	16.10	26.30	32.19	3.26	10.12	0.68	27.48	40.00
	6	3.25	1.17	35.99	0.24	0.44	5.43	14.94	2.50	16.70	0.52	11.80	20.90	33.85	6.46	19.09	1.35	25.65	54.40
	7	2.08	0.78	37.41	0.16	1.07	3.35	10.35	1.83	17.71	0.38	7.90	14.80	34.81	3.97	11.40	0.83	28.48	41.50
		R_s (µmol CO_2 m^{-2} s^{-1})						T_s (°C)						VWC_s (%)					
Hoellengebirge	RecNo	mean	SD	CV	SE	Min	Max	mean	SD	CV	SE	Min	Max	mean	SD	CV	SE	Min	Max
FE	1	1.38	0.59	42.81	0.15	0.69	2.97	12.64	1.78	14.05	0.44	9.60	16.40	32.63	3.89	11.93	0.97	25.81	39.80
	2	0.93	0.42	44.94	0.10	0.25	2.15	13.81	2.66	19.30	0.67	8.60	18.10	33.24	3.37	10.12	0.84	28.65	41.98
	3	4.23	1.47	34.81	0.37	2.02	7.07	14.31	0.62	4.36	0.16	13.50	16.00	40.26	3.27	8.13	0.82	35.23	45.31
	4	7.03	2.33	33.21	0.58	2.84	10.16	18.89	1.00	5.30	0.25	16.90	21.30	34.38	3.22	9.38	0.81	29.23	41.60
	5	5.44	2.75	50.65	0.69	2.15	12.37	18.81	1.26	6.69	0.31	16.10	20.80	30.38	3.70	12.17	0.92	24.98	40.70
	6	4.26	2.33	54.76	0.58	1.26	10.60	14.50	1.24	8.57	0.31	11.90	16.40	30.01	4.20	13.99	1.05	24.48	42.90
	7	2.54	1.03	40.64	0.26	1.20	4.92	12.09	1.36	11.27	0.34	9.10	14.70	32.08	3.23	10.07	0.81	27.31	38.48

Table A2: Summary statistics of campaign wise measured soil respiration (R_s), soil temperature (T_s) and volumetric water content (VWC_s) for the whole site and the unfenced treatment (UF) at the Reutte site.

Reutte		R_s (µmol CO_2 m^{-2} s^{-1})						T_s (°C)						VWC_s (%)					
	RecNo	mean	SD	CV	SE	Min	Max	mean	SD	CV	SE	Min	Max	mean	SD	CV	SE	Min	Max
	1	5.67	2.15	37.85	0.41	2.21	10.04	13.16	1.62	12.30	0.31	10.60	17.20	32.89	5.16	15.70	0.82	23.00	43.90
	2	6.88	2.67	38.77	0.36	2.90	12.12	16.69	2.09	12.51	0.28	13.70	21.10	39.17	3.45	8.81	0.46	29.48	47.70
	3	7.25	3.30	45.53	0.52	1.70	16.47	17.94	1.81	10.07	0.29	15.20	21.90	32.71	4.26	13.02	0.67	25.15	42.40
	4	5.86	3.25	55.49	0.51	1.77	20.64	15.06	1.77	11.74	0.28	12.00	19.50	35.22	5.04	14.31	0.80	25.15	46.10
	5	4.55	2.83	62.36	0.45	1.77	17.99	13.39	1.74	13.02	0.28	9.90	17.20	32.29	5.36	16.61	0.85	24.48	47.20
	6	2.13	1.14	53.56	0.18	0.44	5.68	7.74	1.69	21.88	0.27	5.40	11.90	32.89	5.16	15.70	0.82	23.00	43.90
		R_s (µmol CO_2 m^{-2} s^{-1})						T_s (°C)						VWC_s (%)					
Reutte	RecNo	mean	SD	CV	SE	Min	Max	mean	SD	CV	SE	Min	Max	mean	SD	CV	SE	Min	Max
UF	1	6.28	2.07	32.93	0.53	2.78	10.04	14.23	1.25	8.81	0.32	12.40	17.20	35.61	3.76	10.55	0.97	29.48	43.40
	2	8.79	2.01	22.82	0.49	4.29	12.12	19.41	1.08	5.56	0.26	17.80	21.10	37.02	3.80	10.26	0.92	29.48	45.00
	3	9.17	3.67	40.02	0.92	3.60	16.47	19.72	0.90	4.56	0.22	18.70	21.90	32.93	3.45	10.48	0.86	26.48	38.40
	4	7.67	4.01	52.25	1.00	3.60	20.64	16.21	1.40	8.61	0.35	14.60	19.50	35.41	2.91	8.21	0.73	29.98	40.70
	5	5.58	3.85	68.94	0.96	1.89	17.99	15.00	1.10	7.34	0.28	13.70	17.20	30.57	2.70	8.82	0.67	25.48	35.90
	6	2.30	1.26	54.95	0.32	1.07	5.68	8.16	1.60	19.58	0.40	5.40	10.70	34.19	3.54	10.35	0.88	27.98	42.10

Table A3: Summary statistics of campaign wise measured soil respiration (R_s), soil temperature (T_s) and volumetric water content (VWC_s) for the fenced site (FE) and the mature stand (MS) at the Reutte site.

		R_s (µmol CO_2 m^{-2} s^{-1})						T_s (°C)						VWC_s (%)					
Reutte	RecNo	mean	SD	CV	SE	Min	Max	mean	SD	CV	SE	Min	Max	mean	SD	CV	SE	Min	Max
FE	1	5.06	2.57	50.89	0.91	2.21	9.72	12.26	0.50	4.04	0.18	11.60	13.00	37.94	4.33	11.42	1.53	31.60	43.81
	2	6.73	2.66	39.48	0.51	2.90	11.24	15.20	0.94	6.20	0.18	13.70	17.30	40.54	2.96	7.30	0.57	33.98	47.70
	3	6.23	2.36	37.84	0.59	1.70	10.73	16.58	1.02	6.16	0.26	15.20	18.30	34.16	4.97	14.55	1.24	25.15	42.40
	4	4.88	2.19	44.91	0.55	1.77	9.85	14.94	1.52	10.20	0.38	13.00	17.60	35.33	7.01	19.85	1.75	25.15	46.10
	5	3.71	1.72	46.51	0.43	1.77	6.88	12.64	1.11	8.82	0.28	11.50	15.30	34.18	7.37	21.55	1.84	24.48	47.20
	6	1.90	0.90	47.52	0.23	0.44	3.41	8.17	1.70	20.83	0.43	5.90	11.90	34.10	6.06	17.78	1.52	24.48	43.90

		R_s (µmol CO_2 m^{-2} s^{-1})						T_s (°C)						VWC_s (%)					
Reutte	RecNo	mean	SD	CV	SE	Min	Max	mean	SD	CV	SE	Min	Max	mean	SD	CV	SE	Min	Max
MS	1	4.61	0.37	8.07	0.19	4.99	4.23	10.90	0.26	2.37	0.13	10.60	11.20	39.06	2.33	5.96	1.16	36.10	41.70
	2	4.53	1.18	26.08	0.34	3.41	6.69	16.22	0.96	5.94	0.28	14.90	17.70	39.14	2.47	6.30	0.71	35.50	43.48
	3	5.45	2.34	42.84	0.83	3.09	10.04	17.09	1.37	8.03	0.48	15.70	19.50	29.35	2.18	7.41	0.77	26.50	32.48
	4	4.21	1.22	28.96	0.43	2.15	5.37	13.00	0.60	4.60	0.21	12.00	14.10	34.62	4.19	12.09	1.48	29.10	42.31
	5	4.14	1.55	37.41	0.55	2.10	6.44	11.65	0.99	8.47	0.35	9.90	13.10	31.92	3.65	11.43	1.29	26.50	37.10
	6	2.24	1.37	61.11	0.48	0.95	5.30	6.05	0.48	7.95	0.17	5.40	6.80	27.89	2.70	9.66	0.95	23.00	30.80

Table A4: Treatment-specific effects of fencing on soil temperature (T_s (°C)), soil volumetric water content (VWC_s (%)) and soil CO_2 efflux (R_s (µmol CO_2 m^{-2} s^{-1})), as assessed by t-tests and Tukey´s HSD tests with mixed model structure.

Variable	Hoellengebirge differences		Reutte differences	
Treatment	HF07 - HU07	MS - RF03	RU03 - RF03	RU03 - MS
complete measurement period				
Ts	-0.35 (0.53) n.s.	-0.67 (0.64) n.s.	1.92 (0.52) **	2.58 (0.64) **
VWCs	-2.74 (0.90) **	-2.81 (1.50) n.s.	-2.17 (1.23) n.s.	0.64 (1.51) n.s
Rs	0.47 (0.39) n.s.	-0.80 (0.78) n.s.	1.79 (0.63)**	2.59 (0.78)**
vegetation period				
Ts	-1.70 (0.53) **	-0.34 (0.44) n.s.	2.34 (0.36) **	2.68 (0.44) **
VWCs	-1.59 (1.00) n.s.	-2.10 (1.46) n.s.	-2.60 (1.19) n.s.	-0.50 (1.46) n.s.
Rs	0.93 (0.56) n.s.	-1.05 (0.99) n.s.	2.18 (0.81)**	3.23 (1.00)**

Values in parentheses represent standard error. Significance levels: n.s. - not significant; * = p-value < 0.1 (marginally significant); ** = p-value < 0.05.

Table A5: Treatment specific effects of fencing on autotrophic (R_a (µmol CO_2 m^{-2} s^{-1})) and heterotrophic respiration (R_h (µmol CO_2 m^{-2} s^{-1})), as assessed by t-tests and Tukey´s HSD tests with mixed model structure.

Variable	Hoellengebirge differences		Reutte differences	
	HF07 - HU07	MS - RF03	RU03 - RF03	RU03 - MS
complete measurement period				
Ra	0.25 (0.14)*	0.56 (0.32) n.s.	0.46 (0.26) n.s.	-0.10 (0.32) n.s.
Rh	0.22 (0.25) n.s.	-1.35 (0.46) n.s.	1.31 (0.38) **	2.66 (0.47) **
vegetation period				
Ra	0.65 (0.22) **	0.42 (0.45) n.s.	0.81 (0.37) **	0.39 (0.45) n.s.
Rh	0.28 (0.35) n.s.	-1.63 (0.59) **	1.61 (0.48) **	3.25 (0.59) **

values in parentheses represent standard error. Significance levels: n.s. - not significant; * = p-value < 0.1 (marginally significant); ** = p-value < 0.05.

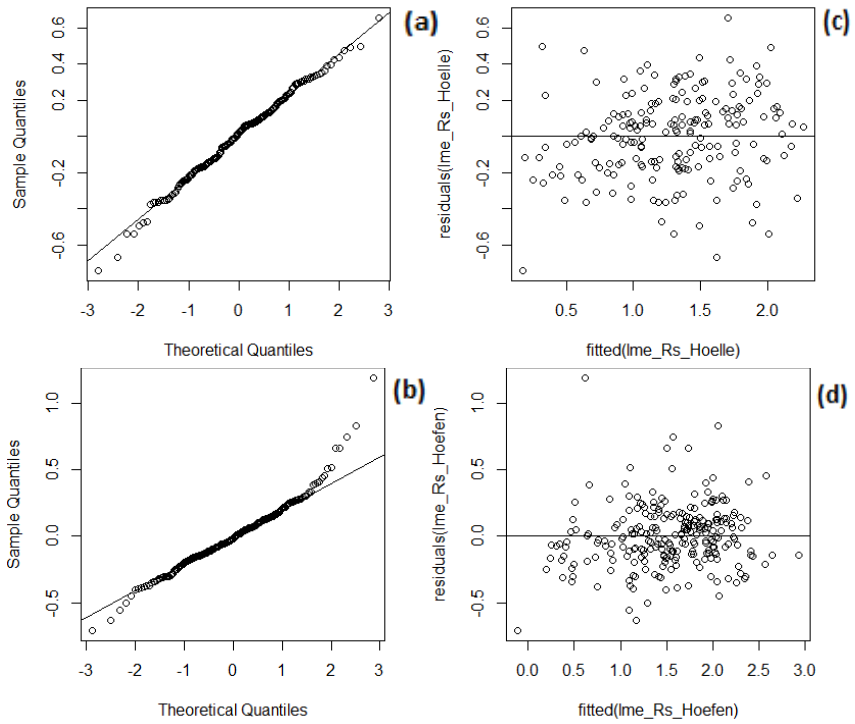

Fig. A1: Model diagnostics of the mixed effects model to predict the soil respiration (µmol CO_2 m^{-2} s^{-1}) in dependence to soil temperature and soil moisture at the specific sampling plots after equation 8 ($Ln(Rs) = \beta 1 + \beta 2\ Ts + \beta 3\ VWCs$) (a & b) Show a QQ - plot of the residuals normality distribution of the model, (c & d) the homoscedasticity plot for the site at the Hoellengebirge and at Reutte, respectively.

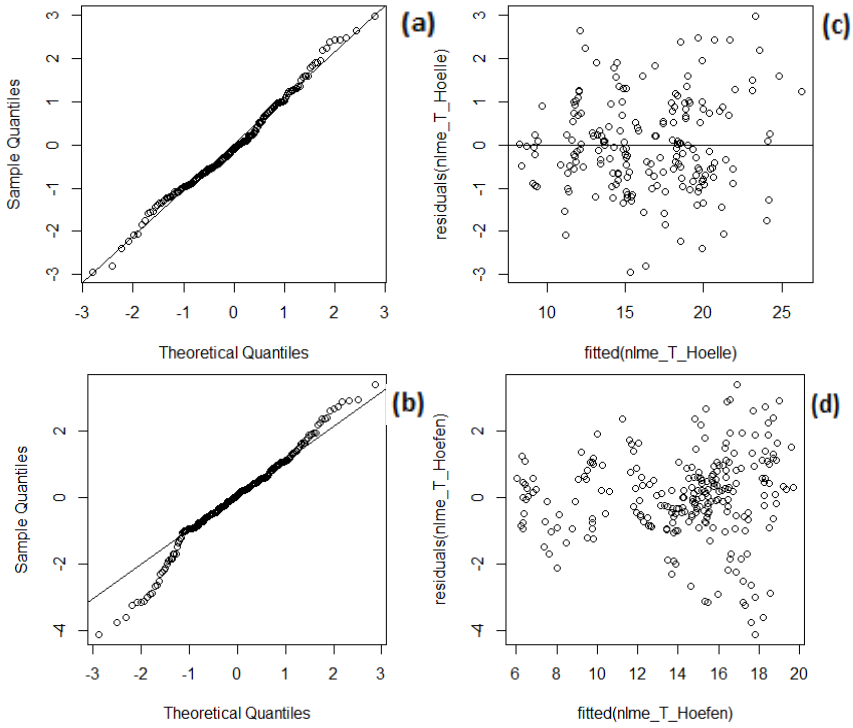

Fig. A2: Model diagnostics of the ME effects model to predict the temperature at 5 cm (°C) at the specific sampling plots after equation 6 ($T_s = \beta_1 + \beta_2\ T_{cont} + \beta_3\ T_{cont}^2$). Quadratic term was included to account for a potential shading effect. (a & b) Show a QQ - plot of the residual normality distribution of the Model, (c & d) the homoscedasticity plot for the site at the Hoellengebirge and at Reutte site, respectively.

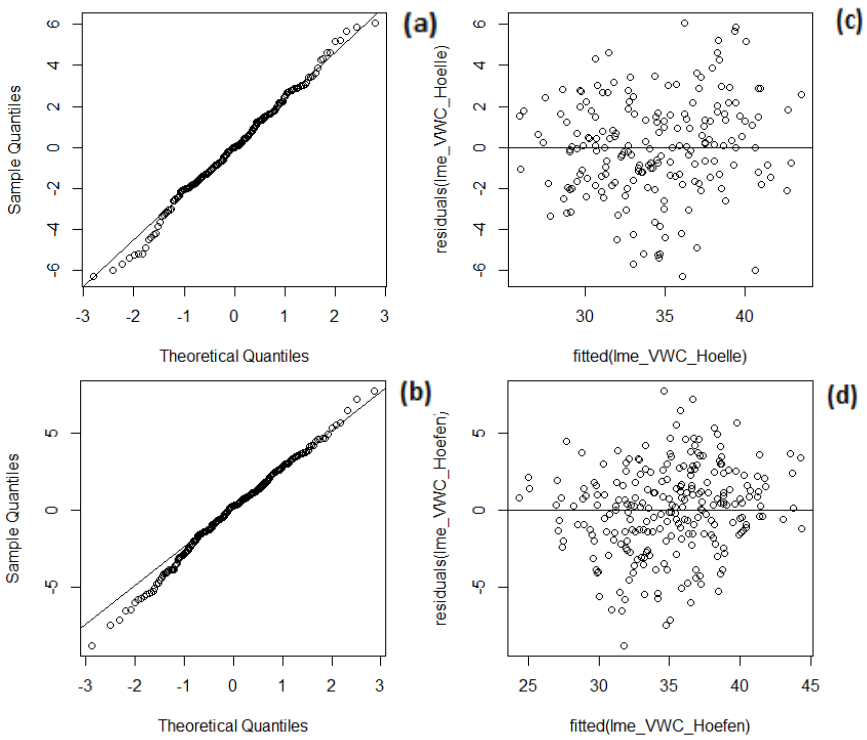

Fig. A3: Model diagnostics of the ME effects model to predict the soil moisture at the specific sampling plots after equation 7 ($VWC_s = \beta_1 + \beta_2\ VWC_{cont}$). (a &b) Show a QQ - plot of the residuals normality distribution of the Model, (c & d) the homoscedasticity plot for the site at the Hoellengebirge and at Reutte, respectively.

Table A6: Summary statistics of campaign wise modeled soil respiration (R_{model}), soil temperature (T_{model}) and volumetric water content (VWC_{model}) for the whole site, the unfenced treatment (UF) and the fenced treatment (FE) at the Hoellengebirge.

Hoellengebirge		R_{model} (µmol CO_2 m^{-2} s^{-1})						T_{model} (°C)						VWC_{model} (%)					
	RecNo	mean	SD	CV	SE	Min	Max	mean	SD	CV	SE	Min	Max	mean	SD	CV	SE	Min	Max
	1	(2.73)	(1.48)	(54)	(0.24)	(0.78)	(8.20)	(10.59)	(1.24)	(12)	(0.20)	(8.63)	(13.33)	(38.79)	(1.94)	(5)	(0.31)	(35.02)	(42.97)
	2	(3.24)	(1.06)	(33)	(0.17)	(1.14)	(5.79)	(10.64)	(0.54)	(5)	(0.09)	(9.47)	(11.74)	(37.76)	(2.32)	(6)	(0.37)	(34.21)	(42.73)
	3	3.98	1.52	38	0.24	1.19	7.48	15.83	1.87	12	0.30	13.26	20.65	39.16	1.97	5	0.32	35.63	43.51
	4	5.46	2.07	38	0.34	1.29	9.67	20.49	2.08	10	0.34	17.20	26.27	33.61	2.69	8	0.44	29.21	39.69
	5	5.02	1.76	35	0.28	1.65	8.78	19.43	1.93	10	0.31	16.11	24.25	30.84	2.97	10	0.47	25.96	37.25
	6	3.29	1.07	33	0.17	1.38	5.55	14.95	1.69	11	0.27	12.30	18.93	32.26	2.75	9	0.45	27.75	38.30
	7	2.50	0.85	34	0.14	1.21	4.41	10.98	1.27	12	0.20	8.28	12.46	35.92	2.34	7	0.38	31.86	40.80

		R_{model} (µmol CO_2 m^{-2} s^{-1})						T_{model} (°C)						VWC_{model} (%)					
Hoellengebirge	RecNo	mean	SD	CV	SE	Min	Max	mean	SD	CV	SE	Min	Max	mean	SD	CV	SE	Min	Max
UF	1	(3.05)	(1.72)	(56)	(0.36)	(0.78)	(8.20)	(9.86)	(0.90)	(9)	(0.19)	(8.63)	(11.55)	(39.23)	(2.03)	(5)	(0.42)	(35.02)	(42.97)
	2	(2.77)	(0.80)	(29)	(0.17)	(1.14)	(4.02)	(10.86)	(0.35)	(3)	(0.07)	(10.23)	(11.74)	(37.63)	(2.67)	(7)	(0.56)	(34.21)	(42.73)
	3	3.80	1.54	41	0.32	1.19	7.20	16.57	2.13	13	0.44	13.26	20.65	39.52	2.04	5	0.43	35.63	43.51
	4	5.15	2.02	39	0.43	1.29	8.34	21.24	2.31	11	0.49	18.19	26.27	34.24	2.69	8	0.57	29.76	39.69
	5	4.79	1.77	37	0.37	1.65	8.78	20.17	2.15	11	0.45	16.11	24.25	31.52	2.97	9	0.62	25.96	37.13
	6	3.07	0.95	31	0.20	1.38	4.80	15.17	2.10	14	0.45	12.30	18.93	32.90	2.72	8	0.58	28.86	38.30
	7	2.18	0.72	33	0.15	1.21	3.78	10.43	1.39	13	0.29	8.28	12.19	36.54	2.27	6	0.47	32.50	40.80

		R_{model} (µmol CO_2 m^{-2} s^{-1})						T_{model} (°C)						VWC_{model} (%)					
Hoellengebirge	RecNo	mean	SD	CV	SE	Min	Max	mean	SD	CV	SE	Min	Max	mean	SD	CV	SE	Min	Max
FE	1	(2.26)	(0.91)	(40)	(0.23)	(1.22)	(4.59)	(11.63)	(0.86)	(7)	(0.21)	(10.19)	(13.33)	(38.16)	(1.67)	(4)	(0.42)	(35.68)	(40.58)
	2	(3.91)	(1.03)	(26)	(0.26)	(2.04)	(5.79)	(10.33)	(0.61)	(6)	(0.15)	(9.47)	(11.43)	(37.95)	(1.78)	(5)	(0.44)	(36.56)	(41.95)
	3	4.24	1.50	35	0.38	2.02	7.48	14.78	0.44	3	0.11	13.98	15.44	38.64	1.81	5	0.45	35.92	42.87
	4	5.88	2.13	36	0.53	2.52	9.67	19.45	1.11	6	0.28	17.20	21.85	32.74	2.50	8	0.63	29.21	39.42
	5	5.36	1.75	33	0.44	2.49	8.10	18.35	0.75	4	0.19	16.82	19.97	29.87	2.76	9	0.69	26.02	37.25
	6	3.59	1.19	33	0.30	1.57	5.55	14.64	0.85	6	0.21	13.11	16.39	31.39	2.63	8	0.66	27.75	38.27
	7	2.96	0.84	28	0.21	1.35	4.41	11.77	0.36	3	0.09	11.18	12.46	35.01	2.20	6	0.55	31.86	40.61

Table A7: Summary statistics of campaign wise modeled soil respiration (R_{model}), soil temperature (T_{model}) and volumetric water content (VWC_{model}) for the whole site and the unfenced treatment (UF) at the Reutte site.

Reutte		R_{model} (µmol CO_2 m^{-2} s^{-1})						T_{model} (°C)						VWC_{model} (%)					
	RecNo	mean	SD	CV	SE	Min	Max	mean	SD	CV	SE	Min	Max	mean	SD	CV	SE	Min	Max
	1	4.59	1.34	29	0.26	1.84	6.95	12.79	1.87	15	0.36	9.23	15.59	37.64	1.95	5	0.38	32.69	41.84
	2	6.80	2.44	36	0.33	3.18	13.96	16.07	1.34	8	0.18	14.16	18.73	37.69	2.63	7	0.48	32.09	44.37
	3	7.36	2.97	40	0.47	3.22	18.74	17.54	1.37	8	0.22	15.13	19.71	31.61	4.25	13	0.67	24.37	43.02
	4	5.52	2.15	39	0.34	2.06	13.06	15.06	1.49	10	0.24	12.10	17.46	34.68	3.27	9	0.52	29.08	43.71
	5	4.28	1.80	42	0.29	1.68	8.09	14.72	2.21	15	0.35	10.39	18.58	33.44	3.79	11	0.60	27.12	43.54
	6	2.23	0.89	40	0.14	0.90	4.38	7.92	1.42	18	0.22	6.04	10.19	34.82	3.26	9	0.52	28.91	43.76
		R_{model} (µmol CO_2 m^{-2} s^{-1})						T_{model} (°C)						VWC_{model} (%)					
Reutte	RecNo	mean	SD	CV	SE	Min	Max	mean	SD	CV	SE	Min	Max	mean	SD	CV	SE	Min	Max
UA	1	5.03	1.11	22	0.29	3.36	6.76	13.47	1.73	13	0.45	11.24	15.59	37.51	2.00	5	0.52	32.69	41.84
	2	9.03	2.49	28	0.60	4.79	13.96	17.71	0.91	5	0.22	16.32	18.73	36.60	2.56	7	0.62	32.09	41.41
	3	9.44	3.11	33	0.78	4.38	18.74	18.72	0.58	3	0.15	17.72	19.71	31.42	2.81	9	0.70	25.09	35.70
	4	6.71	2.22	33	0.55	2.97	13.06	16.30	0.75	5	0.19	14.86	17.46	34.31	2.31	7	0.58	29.08	38.83
	5	5.15	1.96	38	0.49	2.44	8.09	16.87	1.20	7	0.30	13.70	18.58	33.12	2.49	8	0.62	27.45	37.42
	6	2.48	0.91	37	0.23	1.27	4.38	8.28	1.47	18	0.37	6.24	9.75	34.39	2.37	7	0.59	28.91	38.67

Table A8: Summary statistics of campaign wise modeled soil respiration (R_{model}), soil temperature (T_{model}) and volumetric water content (VWC_{model}) for the fenced treatment (FE) and the mature stand (MS) at the Reutte site.

		R_{model} (µmol CO_2 m^{-2} s^{-1})						T_{model} (°C)						VWC_{model} (%)					
Reutte FE	RecNo	mean	SD	CV	SE	Min	Max	mean	SD	CV	SE	Min	Max	mean	SD	CV	SE	Min	Max
	1	4.02	1.69	42	0.60	1.84	6.95	13.03	0.74	6	0.26	11.92	14.00	36.79	1.30	4	0.46	34.83	39.22
	2	6.04	1.82	30	0.35	3.18	8.57	15.15	0.63	4	0.12	14.16	16.50	39.02	2.73	7	0.53	34.80	44.37
	3	6.13	2.13	35	0.53	3.22	10.09	16.78	1.21	7	0.30	15.37	18.73	32.90	5.71	17	1.43	24.37	43.02
	4	5.08	1.90	37	0.48	2.06	8.97	14.80	0.99	7	0.25	13.66	16.53	35.83	4.26	12	1.07	29.65	43.71
	5	3.73	1.57	42	0.39	1.68	6.43	13.17	0.81	6	0.20	11.78	14.42	34.62	5.12	15	1.28	27.12	43.54
	6	2.05	0.82	40	0.20	0.90	3.76	8.12	1.40	17	0.35	6.37	10.19	36.01	4.23	12	1.06	29.89	43.76

		R_{model} (µmol CO_2 m^{-2} s^{-1})						T_{model} (°C)						VWC_{model} (%)					
Reutte MS	RecNo	mean	SD	CV	SE	Min	Max	mean	SD	CV	SE	Min	Max	mean	SD	CV	SE	Min	Max
	1	4.07	0.91	22	0.45	2.86	4.92	9.76	0.41	4	0.21	9.23	10.24	39.85	1.32	3	0.66	38.28	41.46
	2	5.34	1.28	24	0.37	4.33	7.75	15.81	0.73	5	0.21	14.70	16.89	36.66	1.16	3	0.33	35.15	38.82
	3	5.66	1.48	26	0.52	3.87	7.67	16.68	1.11	7	0.39	15.13	18.43	29.42	2.11	7	0.75	26.95	32.36
	4	4.02	1.09	27	0.38	2.99	5.83	13.09	1.00	8	0.35	12.10	15.01	33.13	1.80	5	0.64	31.06	36.03
	5	3.62	1.28	36	0.45	1.93	5.54	13.51	2.24	17	0.79	10.39	16.00	31.74	1.95	7	0.69	29.59	34.53
	6	2.11	0.99	47	0.35	1.21	4.20	6.80	0.74	11	0.26	6.04	8.01	33.33	1.62	5	0.57	31.49	35.87

Table A9: Modeled amount of total emitted carbon (gC m^{-2}) for the different locations and treatments during the measurement period from 18.06.2016 to 24.10.2016

Location	Treatment	Respiration	C efflux (gC m^{-2})		SE
Hoellengebirge	UF	R_s	404	±	26
	UF	R_h	255	±	17
	UF	R_a	149	±	9
	FE	R_s	460	±	38
	FE	R_h	299	±	26
	FE	R_a	160	±	12
Reutte	UF	R_s	727	±	58
	UF	R_h	498	±	31
	UF	R_a	229	±	29
	FE	R_s	501	±	43
	FE	R_h	328	±	27
	FE	R_a	173	±	17
	MS	R_s	521	±	55
	MS	R_h	264	±	26
	MS	R_a	257	±	29

Table A10: Summary statistics of post-hoc Tukey tests for a further subdivision of the factor variables "Stratum" and "Humus form" and two sample t-test for the factor variable "soil group" with respect to R_{10}. Significant p-values are highlighted in bold ($p < 0.05$)

Variable comparison		difference	lower	upper	p-value
a) Treatment	RF03-RU03	-0.723	-1.439	-0.007	**0.047**
	MS-RU03	-0.307	-1.031	0.416	0.575
	MS-RF03	0.416	-0.319	1.150	0.375
		difference	lower	upper	p-value
b) Humus form	Mull-Moder	0.608	0.010	1.207	**0.049**
	Tangel-Moder	-0.158	-2.257	1.942	0.968
	Tangel-Mull	-0.766	-2.858	1.326	0.550
		mean	t-value	degrees of freedom	p-value
c) Soil group	Mineral	3.865	4.355	143	**< 0.001**
	Organic	2.773			

Table A11: Summary statistics of post-hoc Tukey tests for a further subdivision of the factor "Canopy Cover" and "Functional group" with respect to measured soil temperature. Significant p-values are highlighted in bold ($p < 0.05$).

Variable comparison		difference	lower	upper	p-value
a) Canopy closure	high-low	-1.085	-3.759	1.590	0.723
	no canopy cover - low	1.056	-1.677	3.789	0.752
	medium - low	-0.518	-3.534	2.499	0.931
	no canopy cover - high	2.141	1.155	3.127	**0.001**
	medium - high	0.567	-1.047	2.180	0.802
	medium - no canopy closure	-1.574	-3.282	0.134	**0.043**
		difference	lower	upper	p-value
b) Functional group	decidious-coniferous	1.096	-0.267	2.458	0.489
	grass-coniferous	2.482	1.199	3.764	**0.001**
	herbs-coniferous	3.529	0.256	6.802	**0.025**
	moss-coniferous	1.151	-1.111	3.412	0.741
	rubus-coniferous	1.117	-1.942	4.176	0.934
	shrubs-coniferous	3.887	0.919	6.855	**0.002**
	grass-decidious	1.386	-0.155	2.927	**0.048**
	herbs-decidious	2.433	-0.949	5.816	0.337
	moss-decidious	0.055	-2.362	2.472	1.000
	rubus-decidious	0.021	-3.155	3.197	1.000
	shrubs-decidious	2.791	-0.297	5.880	0.107
	herbs-grass	1.047	-2.304	4.398	0.968
	moss-grass	-1.331	-3.704	1.042	0.643
	rubus-grass	-1.365	-4.508	1.778	0.858
	shrubs-grass	1.405	-1.649	4.459	0.822
	moss-herbs	-2.379	-6.212	1.455	0.524
	rubus-herbs	-2.412	-6.765	1.940	0.656
	shrubs-herbs	0.358	-3.931	4.646	1.000
	rubus-moss	-0.034	-3.687	3.619	1.000
	shrubs-moss	2.736	-0.841	6.313	0.264
	shrubs-rubus	2.770	-1.358	6.898	0.425